A Bayesian approach to understanding the key factors influencing temporal variability in stream water quality: a case study in the Great Barrier Reef catchments

Shuci Liu[1*], Dongryeol Ryu[1], J. Angus Webb[1], Anna Lintern[1,2], Danlu Guo[1], David Waters[3], Andrew W. Western[1]

[1]Department of Infrastructure Engineering, The University of Melbourne, Parkville, VIC, 3010.
[2]Department of Civil Engineering, Monash University, VIC, 3800.
[3]Queensland Department of Natural Resources, Mines and Energy, Toowoomba, QLD, 4350.

Correspondence to: Shuci Liu (shucil@student.unimelb.edu.au)

Abstract. Stream water quality is highly variable both across space and time. Water quality monitoring programs have collected a large amount of data that provide a good basis to investigate the key drivers of spatial and temporal variability. Event-based water quality monitoring data in the Great Barrier Reef catchments in northern Australia provides an opportunity to further our understanding of water quality dynamics in sub-tropical and tropical regions. This study investigated nine water quality constituents, including sediments, nutrients and salinity, with the aim of: 1) identifying the influential environmental drivers of temporal variation in flow event concentrations; and 2) developing a modelling framework to predict the temporal variation in water quality at multiple sites simultaneously. This study used a hierarchical Bayesian model averaging framework to explore the relationship between event concentration and catchment-scale environmental variables (e.g., runoff, rainfall and groundcover conditions). Key factors affecting the temporal changes in water quality varied among constituent concentrations, as well as between catchments. Catchment rainfall and runoff affected in-stream particulate constituents, while catchment wetness and vegetation cover had more impact on dissolved nutrient concentration and salinity. In addition, in large dry catchments, antecedent catchment soil moisture and vegetation had a large influence on dissolved nutrients, which highlights the important effect of catchment hydrological connectivity on pollutant mobilisation and delivery.

1 Introduction

In-stream water quality plays a vital role in influencing the health of freshwater ecosystems (Pérez-Gutiérrez et al., 2017), which in turn underpins environmental, social and economic sustainability (McGrane, 2016; Ustaoğlu et al., 2020). Pollution derived from agricultural land and urban development has led to water quality degradation in streams and lakes in many regions of the world (Ren et al., 2003). Among these water quality issues, coastal regions with high agricultural production have been delivering large amounts of pollutants to the ocean, where marine ecosystems are vulnerable to the evaluated levels of nutrients and sediments (Gorman et al., 2009). It is estimated that 60% of coastal rivers in the USA have been

moderately to severely degraded (Gorman et al., 2009; Howarth et al., 2002). Therefore, to protect both freshwater and marine ecosystems, better management of catchment-derived pollutants is needed.

Surface water quality is highly variable across spatial and temporal scales (Guo et al., 2019; Lintern et al., 2018a). These spatial and temporal variations are the result of complex interactions between three key pollutant processes in catchments, namely, sources (e.g., atmospheric deposition or anthropogenic inputs), mobilisation (e.g., detachment from the sources), ~~and~~ delivery (e.g., transport from sources to receiving waters) and transformation (e.g., biogeochemical processes) (Granger et al., 2010; Harris, 2001; Lintern et al., 2018a). Across different catchments, spatial differences in water quality concentration can vary markedly due, in part, to heterogeneity of natural landscapes in catchments (e.g., geology, topography and climate) and human-induced activities (e.g., agricultural and urban development) (Liu et al., 2018; Mainali et al., 2019). At a site, water quality concentrations can also exhibit significant daily, event, seasonal and annual variability, driven by variations in climatic conditions, in-stream biogeochemical processes and hydrological transport (Thompson et al., 2011). Thus, it can be challenging to design effective catchment water quality management strategies without a sound understanding of the spatial and temporal variation in water quality and the associated driving factors.

While it has been acknowledged that both spatial and temporal variations in water quality are of great importance for effective water resources management (Guo et al., 2020), this study focused on identifying key drivers of the temporal variability in water quality. It follows our previous study investigating spatial variation in water quality in the same region (Liu et al., 2018). A wide range of environmental factors may affect temporal changes in water quality. Runoff and rainfall have been considered as important factors and the most commonly used explanatory variables to describe temporal variation in water quality (Deletic et al., 1998), for example early work by Hem (1948) and Walling (1984). Studies considering hydrometeorological drivers have been typically related to the mobilisation and delivery of pollutants. Catchment soil moisture and evapotranspiration can also have an important role in determining the hydrological cycle (e.g., runoff generation), such as sediments (Bieger et al., 2014), nutrients (Lam et al., 2010) and salinity (Brevik et al., 2006; Tweed et al., 2007), thereby affecting the surface water quality. In addition, riverine water quality has been found to be strongly influenced by seasonal changes in vegetation cover (de Mello et al., 2018; Griffith et al., 2002; Shi et al., 2017). For instance, satellite-derived vegetation indices have provided an opportunity to explore the relationship between land cover and water quality temporal dynamics (Griffith, 2002; Singh et al., 2013). Even though significant research efforts have been made to explore the relationship between water quality and these environmental conditions, a comprehensive understanding of their relative importance in diverse environments and at large scales is still lacking.

Process-based and s~~S~~tatistical modelling approaches ha~~s~~ves been widely used to investigate water quality temporal dynamics in response to changes in the abovementioned environmental factors (Fu et al., 2019; Wellen et al., 2015). Process-based water quality models use complex mass-balance structures, describing the water quality source, mobilisation and transport processes (Abbott et al., 1986; Merritt et al., 2003). They are typically based on hydrological and biogeochemical processes that can affect the generation and transport of pollutants into receiving waters. These models (e.g., Soil and Water Assessment Tool – SWAT, and Source Catchments) have been applied to assess the impact of land use management and

climate on sediment and pollutant concentrations (Arnold et al., 2005; Francesconi et al., 2016; Qi et al., 2018), optimise water management and delivery for agriculture, industry and environmental uses (Ly et al., 2019), and estimate pollutant generation, loss and transport processes (Jayakrishnan et al., 2005; McCloskey et al., 2021). However, the complexity of process-based models results in intensive data and calibration requirements, and large-scale application has been limited (Abbaspour et al., 2015; Arnold et al., 2005). These models may also have large uncertainties in the interpretability of the parameters and their characterization of the effects of specific processes (Wade et al., 2002), such as denitrification in streams (Filoso et al., 2004).

On the other hand, statistical water quality models have a relatively simple mathematical structure, an ability to quantify predictive uncertainty (Kasiviswanathan et al., 2013; Srivastav et al., 2007) and low requirement for *a priori* information on distinct processes (Letcher et al., 2002; Mainali et al., 2019; Schwarz et al., 2006). However, existing statistical water quality modelling studies have limitations. Firstly, water quality monitoring data have often been limited to low sampling frequencies, typically using monthly grab samples. This can result in a lack of information on water quality dynamics over runoff/storm events, which is when a significant proportion of nutrients and sediment loads are transported (Lloyd et al., 2016; Sherriff et al., 2015). Secondly, most studies on statistical water quality modelling have only investigated the relationship between water quality and explanatory variables in a single or limited number of catchments in small regions (Chang et al., 2015; Khan et al., 2020; Koci et al., 2020). Few studies have investigated water quality at multiple locations using the same modelling framework. Lastly, studies have usually relied on a single 'best' model with an assumption that it best approximated the true drivers of water quality (Paliwal et al., 2007; Zhang et al., 2009). This ignores the issue of selection uncertainty. Furthermore, relying on a single model structure might result in misleading conclusions or overconfidence in the results (Wintle et al., 2003).

This study attempted to address these knowledge gaps in statistical water quality models, taking advantages of event-based water quality monitoring data from the Great Barrier Reef (GBR) catchments in northern Australia, where land-derived pollutants have posed threats to ecosystem health of the GBR lagoon (Brodie et al., 2012; McKergow et al., 2005b). We address the limitations in statistical water quality models by using: 1) Bayesian hierarchical modelling was used to investigate water quality ~~spatial and~~ temporal variation, which~~. This~~ allowed the prediction of water quality in multiple catchments, as well as simultaneously quantifying parameter uncertainty (Gelman et al., 2013; Rode et al., 2010; Webb et al., 2009); and 2)~~. In addition, we used~~ Bayesian model averaging (BMA) approaches were used to identify the relative importance of the different environmental factors and provide multi-model weighted predictions, which have been shown to better quantify the uncertainty arising from model selection (Höge et al., 2019; Raftery et al., 1997; Wang et al., 2012). We targeted nine common water quality indicators, including sediments, nutrients and salinity. This is a subset of the constituents that have been monitored in the GBR water quality monitoring program. Our analyses are conducted on constituents that are of great concern to the coral reef ecosystem (McCloskey et al., 2017), and could provide a useful comprehensive picture on the overall water quality status. Finally, we have constrained the variables to only the 'real parameters' that can be directed measured (with the exception of NO_X), which helps to understand full sediment and nutrient

loads being exported to the GBR lagoon. Overall, this study aimed to: (1) identify the key drivers of temporal variation in water quality; and (2) predict water quality temporal variation using a Bayesian multi-model approach.

2 Materials and methods

2.1 Study area

The GBR catchments, situated in north-eastern Australia (~~Figure 1~~Fig. 1), consist of six natural resource management regions whose streams and rivers discharge into the Great Barrier Reef lagoon. These catchments cover a 437,354 km^2, approximately a quarter of the state of Queensland, and exhibit significant diversity in climatic, geological and topographical landscape characteristics, as well as in land use and land management (Bartley et al., 2018; Gilbert et al., 2001). The GBR catchments range from small, steep, high-energy streams in the wet tropics, which are dominated by sugarcane crops and rainforest, to large inland catchments used for savannah grazing, and crops (e.g., grain) and with extensive low energy floodplains in the dry tropics (Table 1) (Davis et al., 2017; Koci et al., 2019; McKergow et al., 2005a). Spatial and temporal variations in rainfall in the GBR catchments are a major cause of the diversity in land use patterns. Annual rainfall ranges from less than 500 mm in the south-west to more than 8000 mm in the north-east (~~Figure~~ Fig. 2 [c]) (Davis et al., 2017; Kuhnert et al., 2009). Distinct wet (November to April) and dry (May to October) seasons result in high seasonal variation in runoff and El Nino-Southern Oscillation (ENSO) leads to high inter-annual variability (Day et al., 2018). In the dry tropics, a few large events in the wet season contribute the majority of annual runoff, and constant low flow dominates during the dry season (Jarihani et al., 2017).

Thirty-two sites within the GBR catchments were selected as case study catchments (~~Figure 1~~Fig.1 and Table C1 in Appendix C). Previous multivariate analysis of the patterns of time-averaged concentrations indicated that there were two groups of sites (Table 1 and ~~Figure~~ Fig. 2 [a])~~, which was a result of spatial heterogeneity in catchment landscape characteristics (Figure 2 [b], [c] and [d]) (Liu et al., 2018)~~. We found that differences in geographic/hydroclimatic catchment characteristics (Fig. 2 [b], [c] and [d]) are the key factors that distinguished the two clusters of sites (e.g., small wet areas (Cluster 1) near the coast where topography (orography) plays an important role in rainfall generation) (Liu et al., 2018). Such geographic differences also lead to more dispersed sites in the drier area (Cluster 2).

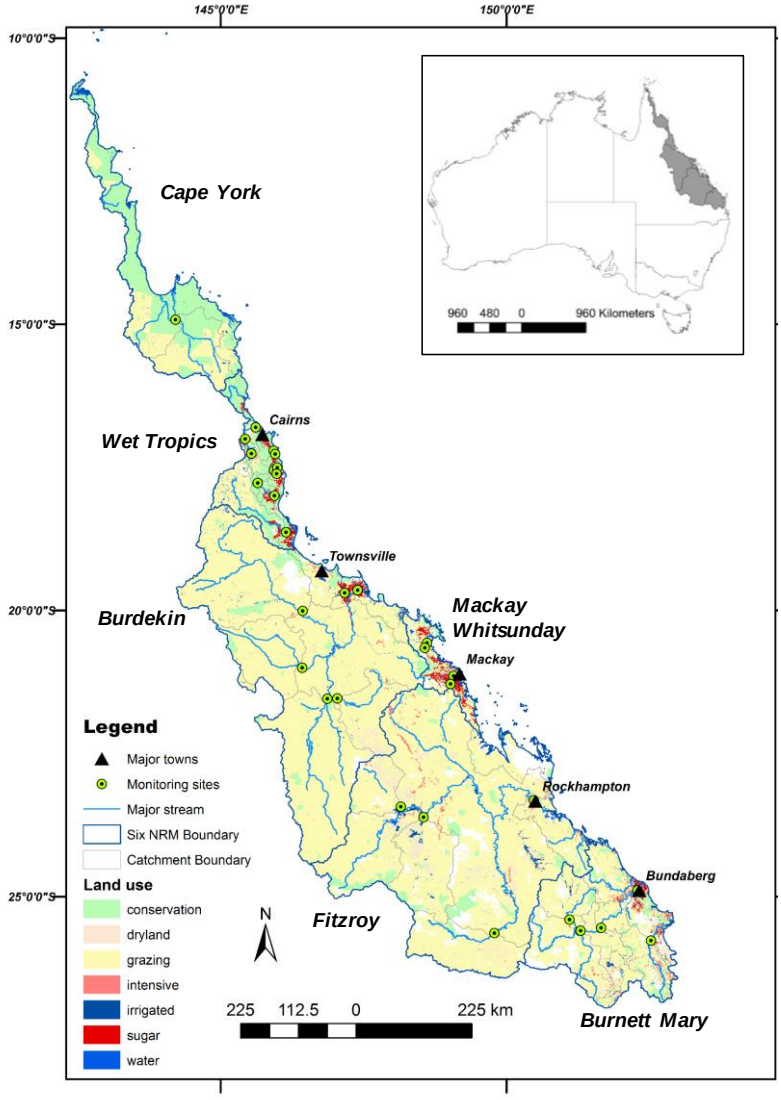

Figure 1: The Great Barrier Reef catchments, monitoring sites, land uses and the six natural resource management (NRM) regions. Land uses have the following characteristics: (1) conservation (forest, woodland, savannah, etc for conservation purposes); (2) dryland (rainfed agriculture including cereals but excluding grazing and sugar cane); (3) grazing (primarily cattle grazing of native and introduced vegetation); (4) intensive (urban areas, roads, etc); (5) irrigated (irrigated cropping excluding sugar cane); (6) sugar (rain-fed and irrigated sugar cane); and (7) water (water bodies, including lake, river, and marsh/wetland).

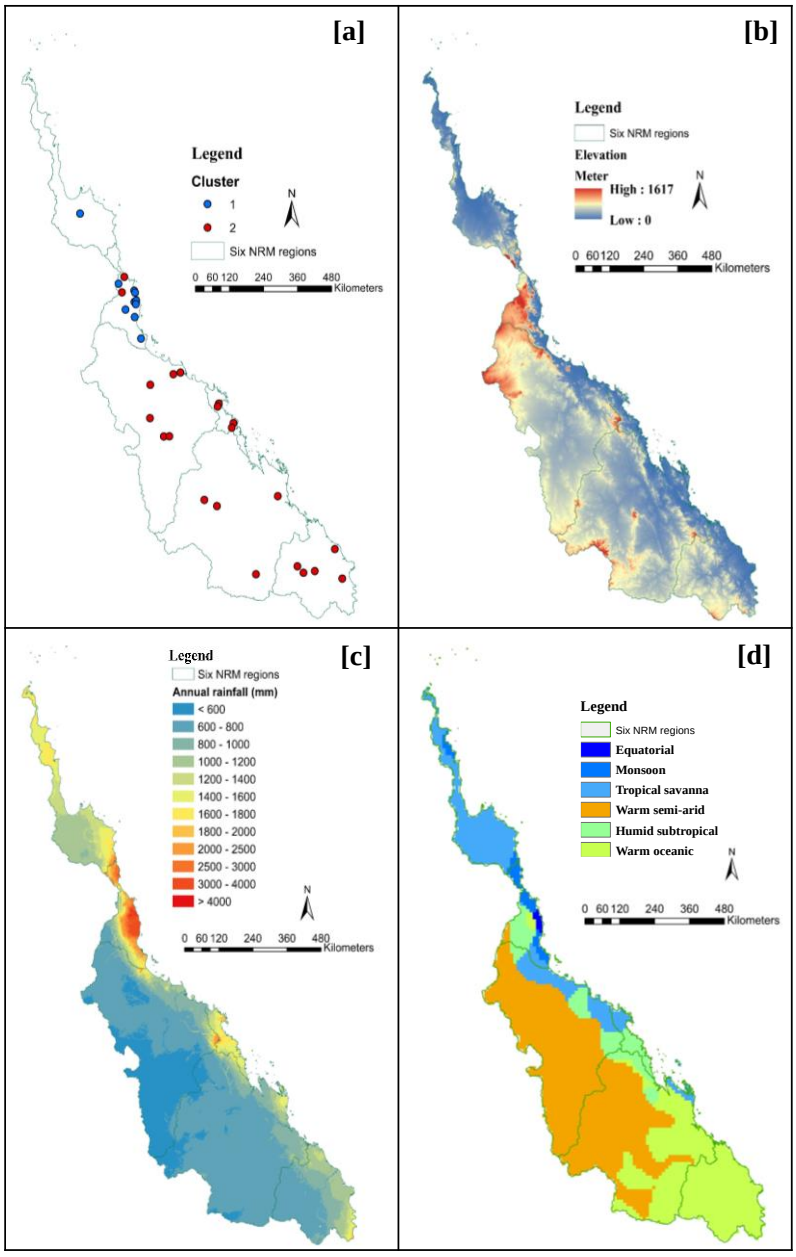

Figure 2: Spatial information of the GBR catchments in northeast of Australia: [a] site locations showing two groups based on clustering analysis of spatial variability in time-averaged water quality (Liu et al., 2018); [b] topographic elevation (250 m resolution) (Geoscience Australia, 2008); [c] annual average rainfall (Bureau of Meteorology, 2012), and [d] updated Köppen-Geiger climate zone classification (Peel et al., 2007).

Table 1: Summary of differences in landscape characteristics between the two clusters of sites (Liu et al., 2018).

Cluster	Climate	Hydrology	Land use/land cover	Topography

1	Wet tropics region with high annual rainfall	Perennial, high energy rivers	Dominated by conservation (e.g., rainforest), and cropping (e.g., sugar)	Small and steep
2	Mostly dry tropics, relatively dry with clear seasonal variability in rainfall	Ephemeral, low energy rivers, cease-to-flow in dry period	Dominated by brigalow native vegetation, and pastures for grazing.	Large and flat

2.2 Data collection and preparation

2.2.1 Water quality data

The nine studied constituents were total suspended solids (TSS), particulate nitrogen (PN), oxidized nitrogen (NO_X), ammonium nitrogen (NH_4), dissolved organic nitrogen (DON), filterable reactive phosphorus (FRP), dissolved organic phosphorus (DOP), particulate phosphorus (PP), and electrical conductivity (EC). Water quality monitoring data collected for the 32 GBR catchments over the 11-year period of 2006 to 2016 were obtained from the Loads Monitoring Program (Turner et al., 2012). This dataset contained both high-frequency event-based samples (e.g., daily or every few hours by automatic samplers) that were taken during runoff events, as well as grab samples (e.g., monthly) that were taken under baseflow conditions (Orr et al., 2014; Waters et al., 2007). As EC data from the Loads Monitoring Program were limited, we extracted additional EC data from the Water Monitoring Information Portal provided by the Department of Natural Resources, Mines and Energy of Queensland (DNRME, 2018) to complement the Loads Monitoring Program records.

2.2.2 Event mean concentration

We extracted continuous discharge records for each site from the Water Monitoring Information Portal (DNRME, 2018) to identify individual runoff events. An automated hydrograph analysis tool – *HydRun* (Tang et al., 2017) was used to delineate runoff events. This approach allowed us to extract runoff event on the baseflow-free hydrograph, by specifying a set of parameters (e.g., β filter coefficient, *ReTh* difference between two flows to set the local minima for event extraction). This toolbox directly returned the start and end points of an event, thereby avoiding time-consuming and subjective inconsistent outcomes. ~~The start and end points of a specific event were determined by using a local minimum method that calculates the first derivative of the streamflow record (separated from baseflow).~~ The key parameters used for *HydRun* Toolbox are provided in Table C2 (Appendix C) and an example hydrograph output is provided in Fig. B1. These parameters are determined based on recommended values from literature (Garzon-Garcia et al., 2016; Ladson et al., 2013; Zhang et al., 2017), as well as manual review of all event hydrographs ensured overall consistency. The event-mean concentration (EMC) was then calculated for each event that had at least two samples on each of the rising and falling limbs of the hydrograph. Thus, for each EMC, a minimum of 4 samples was achieved, which is above the standard (3 samples per event) set by Bartley et al. (2012). On average, there were 14 samples per event across the nine constituents (ranging from 12 for DOP to

16 for EC, Table C3). This ensured that the water quality dynamics over a runoff event were reasonably well-captured, and that the derived EMCs were reliable (Waters et al., 2007). For each event, the EMC of a constituent was calculated as the total load per unit flow volume within the event using (Bartley et al., 2012):

$$EMC = \frac{Event\ Load}{Event\ Flow\ Volume} = \frac{\sum_{j=0}^{n} \frac{c_j + c_{j+1}}{2} \times q_{j+1/2} \times t_{j+1/2}}{\sum_{j=0}^{n} q_{j+1/2} \times t_{j+1/2}} \quad (1)$$

where n is the total number of samples for a given event, c_j is concentration of the j^{th} sample, $q_{j+1/2}$ and $t_{j+1/2}$ are the inter-sample mean discharge and time interval between j^{th} and $(j+1)^{th}$ samples. The concentrations at the start and end of the event (c_0 and c_{n+1}) are assumed to be the averaged value for samples during baseflow (with baseflow identified in the previous section). The EMCs were essentially flow-weighted mean concentrations over individual runoff events, which allowed the comparison of water quality across catchments with contrasting flow regimes (e.g., two clusters of sites in ~~Figure~~ Fig. 2) (Cooke et al., 2000; Richards et al., 1993). A total of 1412 events was identified across the 32 sites, and, depending on data availability, EMCs were calculated for between 21% (DOP) and 43% (TSS) of these identified runoff events (Table C2).

The derived EMCs (i.e., rather than the individual water quality samples) were –Box-Cox transformed to improve the symmetry of the response variable (Box et al., 1964). T~~t~~he normalization of the predictand is necessary to facilitate the fitting process and ~~fulfill~~fulfil the statistical assumption of our model~~;~~. This is because we use a Bayesian linear regression with the response variable sampled from a normal distribution (Sect. 2.3.1) (Atkinson, 2020; Castillo et al., 2015; Hoeting et al., 2002)~~to improve model fitting~~. The site-level Box-Cox transformation parameter λ for each constituent was first identified, using the *car* package in *R* (Fox et al., 2012; R Core Team, 2013). Then, for each constituent, the average λ from the 32 sites was used to transform all available EMCs for that specific constituent. This ensured that an identical transformation parameter was applied across the different sites for each constituent (Guo et al., 2019).

2.2.3 Explanatory variables

This study investigated the effect of various hydrologic, climatic and vegetation cover characteristics for different events. These characteristics included runoff, catchment root zone soil moisture, actual evapotranspiration rainfall, air temperature, and vegetation cover. The continuous streamflow monitoring data, gridded weather and climatic products, and remotely sensed imagery were used to derive catchment average conditions for each event (Table 2).

Table 2~~:~~ Explanatory variables and their data sources.

Explanatory variable	Unit	Spatial resolution	Source
Daily runoff	mm/d	point measurements	Queensland Department of Natural Resources, Mines and Energy (DNRME, 2018). Available from https://water-monitoring.information.qld.gov.au/
Daily rainfall	mm	5 km × 5 km	Australia Water Availability Project (AWAP) (Raupach et al., 2009). Available from http://www.csiro.au/awap/

Daily temperature	°C		
16-day normalized difference vegetation index (NDVI)	-	1 km × 1 km	Moderate Resolution Imaging Spectroradiometer (MODIS) - MOD13A2v006 (Didan, 2015). Available from https://earthdata.nasa.gov/
Daily soil moisture (root zone 0 -100 cm)	mm	5 km × 5 km	Australia Landscape Water Balance model (AWRA-L) (Frost et al., 2016). Available from http://www.bom.gov.au/water/landscape
Daily actual ET	mMm		

Note: ET – evapotranspiration

For individual runoff events identified in the previous section, three groups of event characteristics were prepared, characterising pre-event, during-event and post-event conditions (Table 3). Except for runoff, data for all explanatory variables were first extracted from gridded data using catchment boundaries were delineated using the Geofabric tool provided by the Australian Bureau of Meteorology (Bureau of Meteorology, 2012) (~~Figure 1~~Fig.1). The catchment average time series data were then averaged over the specific time-window related to the event (Table 3).

Table 3: Three groups of event characteristics and averaging method.

Group	Explanatory variable	Abbreviation used in figures and tables in paper	Calculation method
During-event	Average runoff	Event_ave_Q	Average of daily runoff during event
	Maximum runoff	Event_max_Q	Maximum of daily runoff during event
	Average rainfall	Event_ave_P	Average of daily rainfall during event
	Maximum rainfall	Event_max_P	Maximum of daily rainfall during event
	Average temperature	Event_T	Average of daily temperature during event
	Average NDVI	Event_NDVI	Average of NDVI during event
	Average soil moisture	Event_SM	Average of daily soil moisture during event
	Average actual ET	Event_AET	Average of daily actual ET during event
Pre-event	Average runoff	Ante_Q	Average of daily runoff for 7 days prior to event
	Average rainfall	Ante_P	Average of daily rainfall for 7 days prior to event
	Average NDVI	Ante_NDVI	Average of NDVI for 3 months prior to event
	Average soil moisture	Ante_SM	Average of daily soil moisture for 7 days prior to event
	Average actual ET	Ante_AET	Average of actual ET for 7 days prior to event
Post-event	Average runoff	Post_Q	Average of daily runoff for 7 days after event

Note: Q – runoff; P – rainfall; T – temperature; NDVI – normalized difference vegetation index; SM – root zone soil moisture; ET – evapotranspiration.

The explanatory variables in the during-event conditions were averaged over the duration of the event. For the pre-event and post-event conditions, the 7 days prior to and after the event were used as the time-window (except NDVI). The 7-day period was the median of the time of concentration (i.e., the time for runoff to travel from the most remote point of the catchment to

the monitoring site) across all catchments. These were estimated from catchment topography using the Bransby-William's equation, following its wide application in Australian catchments for flood estimation (Pilgrim et al., 1987). The ground cover was quantified by NDVI, an indicator of the biophysical condition of the vegetation canopy (Griffith et al., 2002). Previous studies have also shown that there is a time-lag between water availability and a change in ground cover, which is typically three months for Australian catchments (De Keersmaecker et al., 2015). Therefore, to represent the pre-event ground cover condition, we averaged all available NDVI measurements for three months prior to an event. The runoff after the event (7 days) was also included as an indicator of catchment wetness at the end of the event, to assess if hydrologic condition towards the end of an event influences the temporal variation in water quality.

Similar to the EMCs, all the explanatory variables were Box-Cox transformed following the procedure described in Sect. 2.2.2. In addition, prior to the analyses, both transformed EMCs and explanatory variables were standardized to a mean of zero and standard deviation of one. As such, the magnitude of a coefficient indicates the effect of each predictor relative to other predictors (Wan et al., 2014). The cross-correlation (non-parametric Spearman's Rank correlation coefficient) of all transformed predictors is provided in ~~Figure~~ Fig. ~~B1~~B2, Appendix B. Some of the variables are proxies for the same process, and thus some paired predictors are highly correlated (e.g., pre-event NDVI and event NDVI with Spearman's ρ = 0.97). Freckleton (2011) highlighted that when applying the model averaging approach, it is not safe to simply exclude correlated variables without due consideration of their likely independent effects. In our case, the high correlation among predictors mainly comes from time lag effects between predictors (e.g., pre-event, event and post-event). The relative importance of these predictors provides strong management indication for future water quality management strategies. Therefore, we have not removed any correlated predictors in this analysis. It is likely that different model structures result in similar predictive performance (discussed in the analysis of the results, i.e., Sect. 3.1).

2.3 Modelling: driver identification and water quality prediction using multi-model inference

The statistical analysis and modelling followed several steps (~~Figure 3~~Fig.3). The Bayesian modelling framework was applied to catchments in Clusters 1 and 2 separately. There are strong practical merits in handling the clusters separately. Previous results from clustering analyses on spatial patterns of water quality and catchment characteristics were highly correlated, and that the two clusters had quite different key explanatory variables (Liu et al., 2018). If all the sites were pooled into the same analysis, it would make it more difficult to identify a universal set of key explanatory variables that represent both clusters and likely increase the uncertainty of the coefficients too. The analysis would identify the same key factors identified for the two different clusters. It is important to consider and model these clusters separately so that we can better inform how water quality can be managed in these separate environmental conditions.~~This is because we assumed that the key drivers of temporal variability in water quality would differ between two Clusters due to their differences in land use and climate.~~

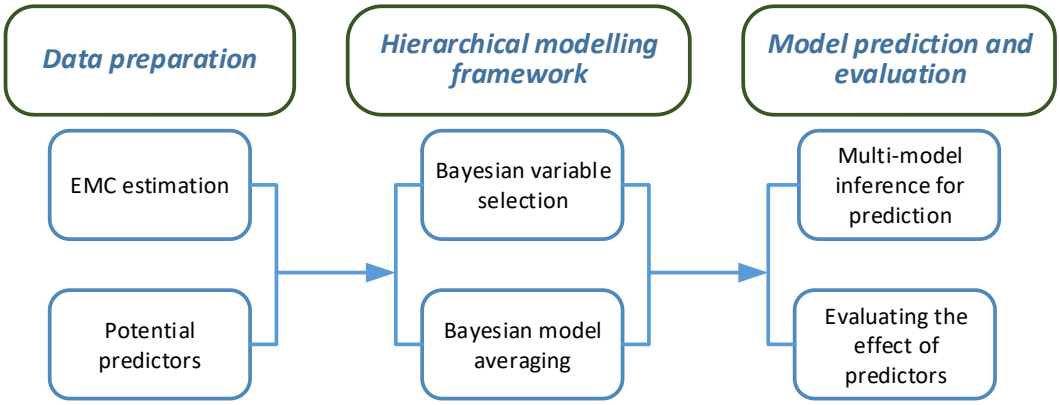

Figure 3: Analyses steps; the detailed methods used in the hierarchical modelling framework and model prediction and evaluation are in the following sections.

2.3.1 Bayesian variable selection

To investigate the relative importance of individual predictors, an indicator Bayesian variable selection method was used called Gibbs variable selection (GVS) (George et al., 1993). An auxiliary inclusion variable I_n (Eq. (2~~(2)~~)) for each predictor was introduced to indicate whether that predictor was 'in' or 'out' of an individual iteration of the hierarchical modelling structure.

$$I_n \begin{cases} 1, & n^{th}\ predictor\ present \\ 0, & n^{th}\ predictor\ absent \end{cases} \quad (2)$$

I_n was modelled at the top level of the hierarchy which enabled the use of identical model structures (i.e., combination of predictors) across different sites. The overarching hierarchical modelling framework was defined as follows:

$$y_{i,j} \sim N(\mu_{i,j}, \sigma) \quad (3)$$

$$\mu_{i,j} = \overline{mean}_j + \overline{std}_j \times \Delta_{i,j} \quad (4)$$

$$\Delta_{i,j} = \sum_{n=1}^{N} \theta_{n,j} \times x_{n,i,j} \quad (5)$$

$$\theta_{n,j} = I_n \times \beta_{n,j} \quad (6)$$

The data-level model (Eq. (3)) assumed that the EMC of a particular constituent (e.g., one of TSS, NO_X, EC, etc) at i^{th} time step in the j^{th} sub-catchment, $y_{i,j}$, followed a normal distribution (denoted as $N(\cdot)$), with mean $\mu_{i,j}$ and a global standard deviation σ. The mean value, $\mu_{i,j}$ was modelled as the observed site-level averaged EMC $\overline{mean}_j$ plus $\overline{std}_j \times \Delta_{i,j}$, with the latter term being defined as the deviation from this averaged value (Eq. (4)) (Guo et al., 2019). The deviation term incorporated the site-level observed standard deviation $\overline{std}_j$, making $\Delta_{i,j}$ a standardised measure that could be compared across sites. $\Delta_{i,j}$ was further modelled as a linear additive function (Eq. (5) of all candidate predictors x_n in n = 1, 2, …, N =

14 (e.g., event average runoff, rainfall and NDVI). Consequently, $\Delta_{i,j}$ was defined as the temporal variability in water quality, and was the quantity of interest. The effect size ($\theta_{n,j}$) of individual predictors was another latent variable used in the GVS, and was estimated as the product of I_n and the regression coefficient $\beta_{n,j}$ (Eq. (6)), such that $\theta_{n,j}$ was either $\beta_{n,j}$ (I_n = 1), or 0 (I_n = 0).

2.3.2 Hierarchical prior specification and Bayesian inference of key drivers

Bayesian inference required specification of prior distributions for each model parameter. We used a hierarchical conditional prior specification for predictor coefficients, allowing the site-specific parameter values that describe the effects of each of the temporal predictors ($\beta_{1,j}, \beta_{2,j\ldots}, \beta_{n,j}$) to be exchangeable between sites (O'Hara et al., 2009; Webb et al., 2009). The detail specification of priors for each model parameter can be found in Appendix A. In addition, to identify key drivers affecting temporal changes in water quality, the posterior inclusion probability (PIP - $P(I_n = 1|y)$, Eq. (A8) in Appendix A) of each predictor was used to compare the relative importance of individual predictors (i.e., how often the n^{th} predictor was 'in' the model).

2.3.3 Prediction from multi-model inference

We used Bayesian Model Averaging to generate an ensemble of predictions of temporal variation in EMC for individual constituents (Eq. (7~~(7~~)). The average posterior distribution of a quantity of interest (i.e., temporal variability in EMC) was generated using the parameters (e.g., $\beta_{1,j}, \beta_{2,j\ldots}, \beta_{n,j}$) sampled from the posterior distribution to simulate EMC values using the specific model, defined as follows:

$$[\hat{y}|y] = \sum_{x=1}^{L} [\hat{y}|y, M_x] P(M_x|y) \quad (7)$$

where $[\hat{y}|y, M_x]$ is the posterior distribution of a vector $\hat{y}$ of (prediction) derived from model M_x, and $P(M_k|\boldsymbol{y})$ is the posterior model probability (PMP, Eq. (A8), in Appendix A) (O'Hara et al., 2009).

2.3.4 Model evaluation and implementation

The proposed modelling framework was applied to the two clusters of sites independently. This allowed an investigation of whether the spatial heterogeneity in catchment landscapes led to differences in the key factors controlling temporal variation in water quality. The key drivers were determined as the predictors with a PIP above 0.8 (i.e., over 80% of the models included these predictors).

To further understand the reliability and robustness of the BMA framework, the consistency of the posterior inclusion probability of individual predictors was investigated by resampling subsets of the observations multiple times (Kohavi, 1995). For each cluster, 80% of events within one site were first randomly selected and the posterior inclusion probability for

this subset of observations was estimated. This was repeated 1,000 times to produce a distribution of posterior inclusion probabilities for individual predictors, which was then used to assess the uncertainty in the posterior inclusion probability.

An ensemble of the averaged prediction in temporal variability of each event was obtained from each iteration of parameter updating using Markov chain Monte Carlo (MCMC). The model fit was evaluated using the Nash-Sutcliffe coefficient (NSE) (Nash et al., 1970) between the observed temporal variability and the median of ensemble predictions $\hat{y}$ derived from the BMA (Eq. (7~~(7~~)). The NSE was calculated at both the cluster- and site-levels. The model residuals were also checked for normality and heteroscedasticity (i.e., relationship between the residual and predictors). In addition, model performance was evaluated by providing the 50% and 95% credible interval (CI) of each prediction.

To compare the relative importance of the predictors that have been widely used in existing literature (i.e., runoff and rainfall) and other predictors (e.g., soil moisture, temperature, evapotranspiration, and vegetation cover), the modelling framework was re-calibrated using only the rainfall/runoff related predictors (including all pre-, during- and post-event predictors). This estimated the degree of improvement in the model's explanatory power with the inclusion of environmental variables, such as catchment wetness and ground vegetation cover conditions.

The hierarchical modelling framework was implemented in *JAGS* (Plummer, 2013a), using the package *rjags* in *R* (Plummer, 2013b; R Core Team, 2013), which enabled both the estimation of parameter values from prior distributions with ~~Markov chain Monte Carlo (~~MCMC~~)~~ and the generation of model-averaged predictions. The MCMC sampling had three parallel chains with 25,000 iterations for each chain. The first 5,000 iterations were discarded as a 'burn-in' period to allow convergence of the Markov chains, resulting in 60,000 values to estimate the posterior distribution for each model parameter and make model predictions.

3. Results

3.1 Key drivers of temporal variability in water quality

The three key measures that were used to quantify the effect of individual predictors are: (1) estimates of posterior inclusion probability (PIP), which quantifies relative importance of individual predictors; (2) posterior model probability (PMP), which estimates differences in plausible model structures; and (3) posterior distributions of coefficients for the key drivers (i.e., effect size, e.g., $\theta_{1,j,}\ \theta_{2,j\ldots,}\ \theta_{n,j}$ in Eq. (6)), which measures direction and magnitude of the effect of key predictors on water quality temporal variability.

Posterior inclusion probability (~~Figure~~ Fig. 4 and Table C3 in Appendix C) from the Bayesian modelling results indicated that, in general, antecedent vegetation condition and antecedent soil moisture were key factors in explaining temporal variation in water quality, especially for Cluster 2 (warmer, drier) sites. Catchment runoff and rainfall were the second most important group of factors, especially for particulate pollutants (TSS, PN and PP; Clusters 1 and 2) and salinity. In addition, the three groups of predictors (pre-, during-, post-event) showed varying effects among the constituents. With regard to

during-event conditions, event average runoff (*Event_ave_Q*), event maximum runoff (*Event_max_Q*) and event average rainfall (*Event_ave_P*) were three important factors with relatively high PIP. In contrast, among pre-event conditions, antecedent NDVI (*Ante_NDVI*) and antecedent soil moisture (*Ante_SM*) were driving factors for the majority of the constituents. Post-event runoff (*Post_Q*) only affected a few constituents (e.g., on NO_X and FRP for Cluster 2), compared with the other two groups of predictors. Overall, there were notable differences in the important predictors for Clusters 1 and 2, and more important predictors were found for the Cluster 2 sites.

It is also worth noting that strong correlations between predictors does not necessary mean that the posterior inclusion probability of these factors is similar (e.g., 1.00 and 0.34 for pre-event NDVI and event NDVI, respectively, for DON in Cluster 2). The BMA can handle the collinearity with shrinking the posterior distribution of inclusion probability of one of the correlated variables towards zero (Nakagawa et al., 2011; Posch et al., 2020; Walker, 2019). This shrinkage effect leads to a lower posterior probability of a more complex model that includes correlated variables, because each extra predictor dilutes the prior density of the existing predictor that it correlates with. Such more complex model is unlikely to be selected, unless the loss in posterior probability can be outweighed by the gain in achieving a higher likelihood (Daoud, 2017; Hinne et al., 2020; Kruschke, 2014).

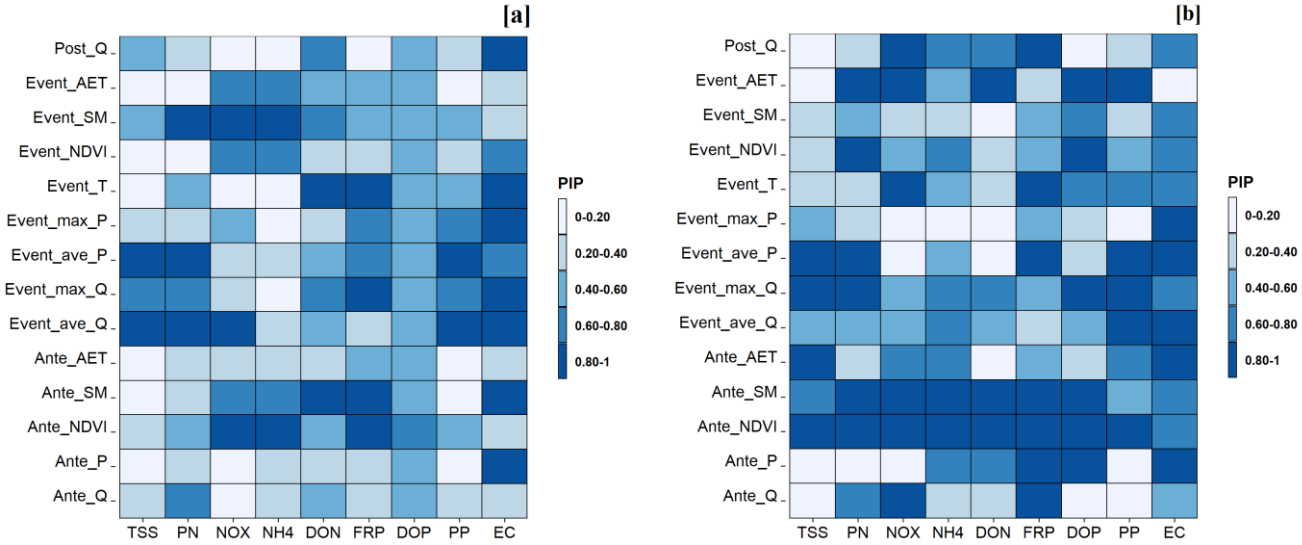

Figure 4: Posterior inclusion probability (PIP) of each candidate predictor for [a] Cluster 1 ("wet") catchments, and [b] Cluster 2 ("dry") catchments; dark blue = high PIP; light blue = low PIP. The definition of the abbreviations of each predictor on the y-axis are in Table 3.

Results from here on will focus mainly on TSS, NO_X and FRP, due to their impacts on the marine receiving environment. Results for the other six constituents are in ~~the Supplementary Materials~~Appendix. Figure 5 shows the posterior model probabilities for TSS, NO_x and FRP for the 100 models with highest PMP (Fig~~ure~~s. ~~B2~~ B3 and ~~B3~~ B4 in Appendix B show

other constituents). Red indicates a negative influence and blue a positive influence. The difference in PIP between the two clusters resulted in quite different plausible model structures (models with relatively high posterior model probability). A stand-out difference between the results for the two Clusters was antecedent vegetation cover condition (*Ante_NDVI*), which tended to be a more important predictor of TSS for Cluster two, than for Cluster one (~~Figure~~ Fig.5 [a]). In addition, the plausible models for Cluster 2 were generally more complex (with a larger number of predictors), expect for DOP and EC (Fig~~ure~~s. ~~B2~~ B3 and ~~B3~~B4).

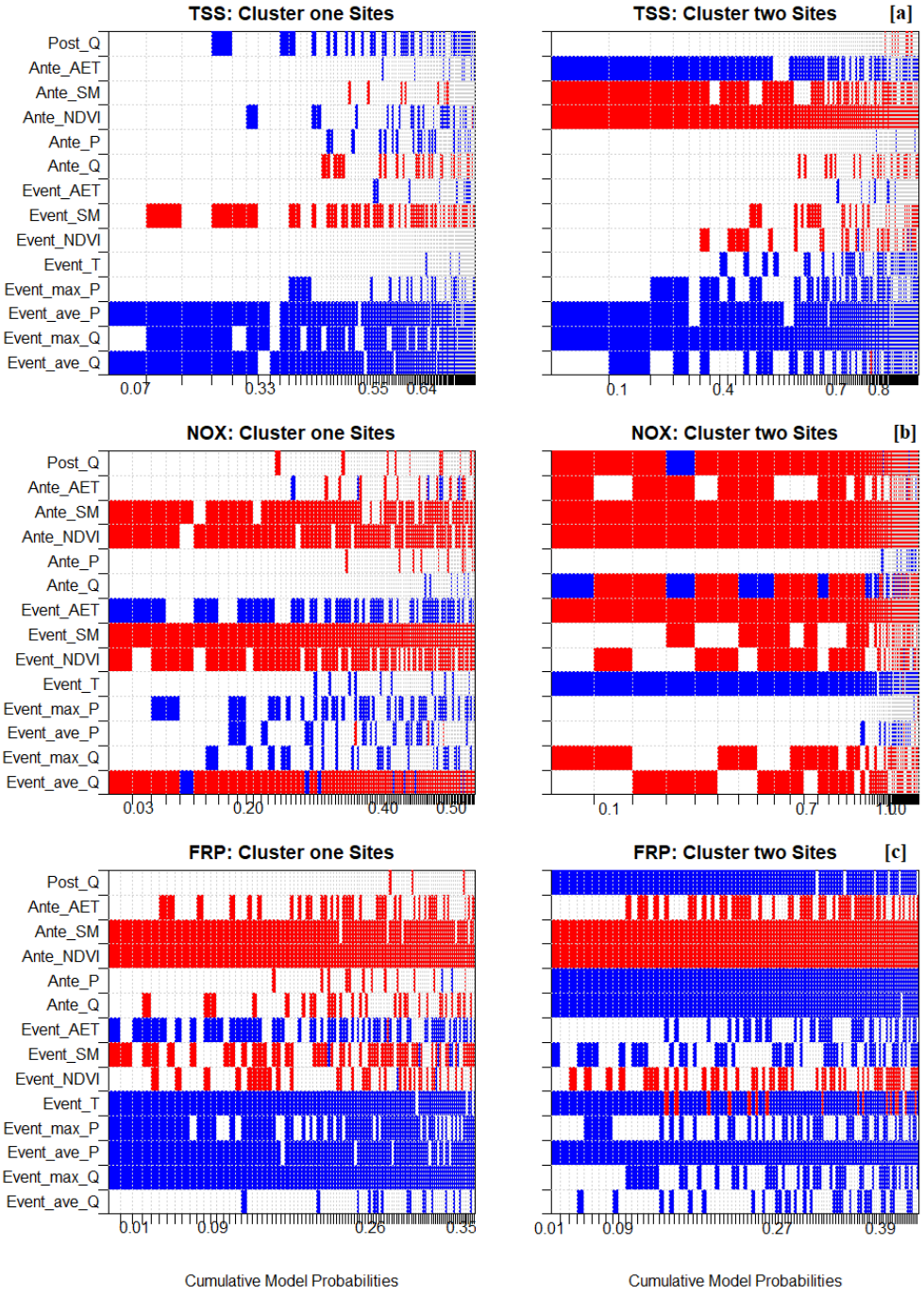

335

Figure 5: Comparison of BMA model coefficients and cumulative model probabilities (only the first 100 models ranked according to the highest probability are shown) between Cluster 1 ("wet" - left) and Cluster 2 ("dry" - right) sites for [a] TSS, [b] NO_X and [c] FRP. ~~The order of predictors on the y-axis was ranked based on the posterior inclusion probability.~~ Each column in the

heatmap represents the one specific model (ranked from highest model probability from left to right) and the width of the column is normalised by the posterior model probability (i.e., the widest columns indicate models with the largest increase in probability compared to the next most probable model). The colour indicates the direction of the coefficients: red = negative; blue = positive. The coefficient value was averaged across the posterior median value of the site-specific coefficient within each cluster (effect size, $\theta_{n,j}$, in Equation 6); the definition of the abbreviations of each predictor on the y-axis are in Table 3.

The distribution of posterior model coefficients for the key predictors (~~Figure 6,~~ Figures 6, ~~B4~~ B5 and ~~B5~~B6) further demonstrated that the key drivers of temporal variability in water quality vary between catchments and between constituents. During-event runoff and rainfall tended to have a positive effect on sediment and particulate constituents and, a negative effect on NO_X and EC. In addition, there was strong negative effect of antecedent vegetation condition on the majority of the constituents.

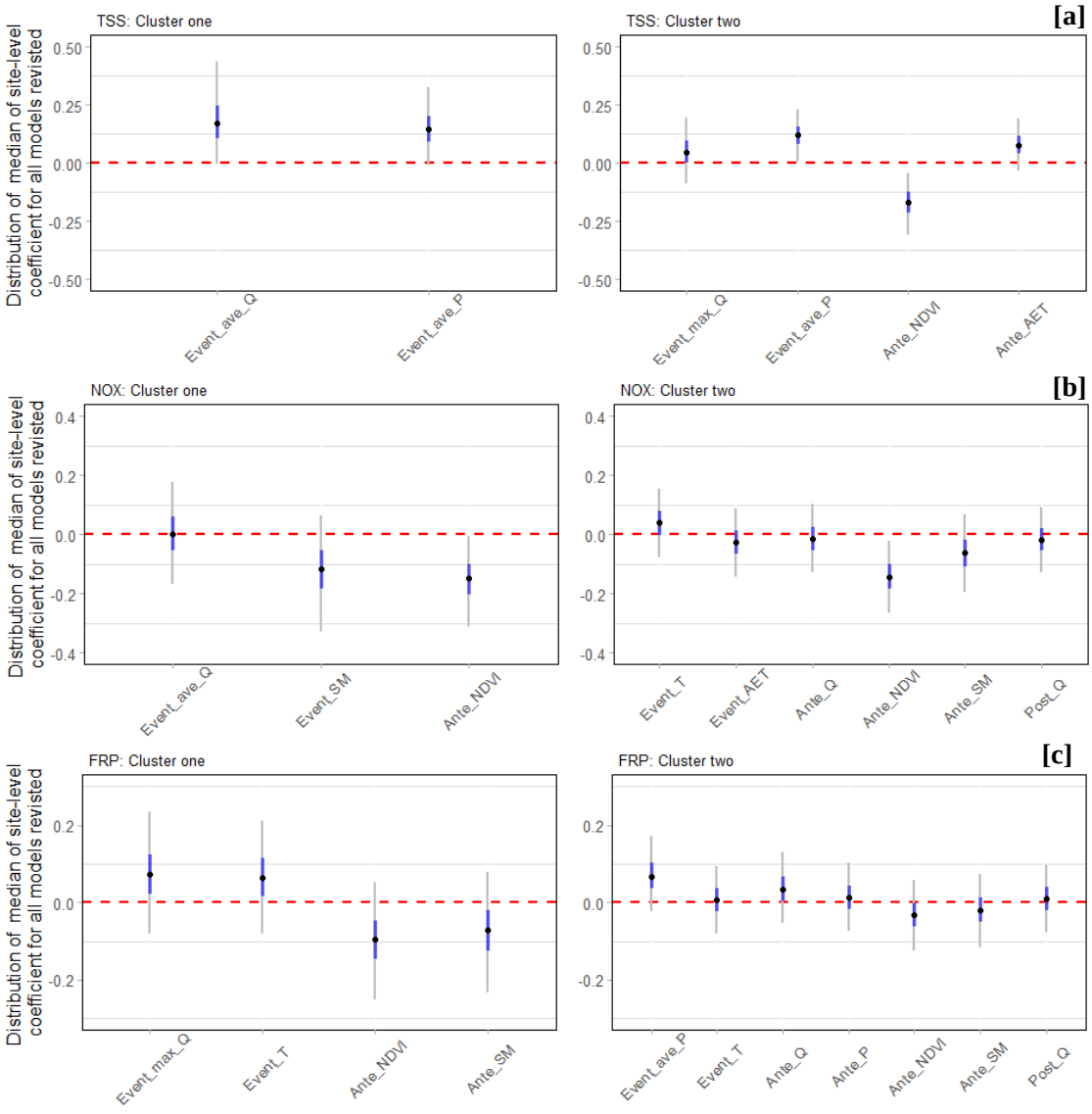

Figure 6: Distribution of median of site-level coefficients for all plausible models in BMA between Cluster 1 ("wet" - left) and Cluster 2 ("dry" - right) sites for: [a] TSS; [b] NO_X and [c] FRP. Only predictors with PIP > 0.8 are included. For each specific model structure, the coefficient value of a predictor was the median of the site-specific coefficient across all sites (effect size, $\theta_{n,j}$, in Eq. (6)). The distribution of this value thus represents the probability of the model (PMP), as well as variability in the same predictor across different sites; black dots = the median; grey vertical lines = 95% CI; blue coloured vertical lines = 50% CI; the definition of the abbreviation of each predictor on x-axis are in Table 3.

The uncertainty in PIP, derived from 1,000 subsampled BMA runs (~~Figure~~ Figs.7, ~~Figures B6~~ B7 and ~~B7~~B8) highlighted that the BMA results were robust for most constituents, except for EC (~~Figure~~ Fig. B7 [c]). BMA tends to identify important predictors and less sensitive to the input data which is evidenced by the relatively narrow range of interquartile ranges (IQR), when PIP for a specific predictor~~s~~ is large (e.g., antecedent soil moisture for FRP in ~~Figure~~ Fig. 7). It is also worth noting that large uncertainty in the PIP for EC was observed, indicating the BMA results were sensitive to the observations of EC. This might be related to data availability, which is further discussed in Sect. 4.2.

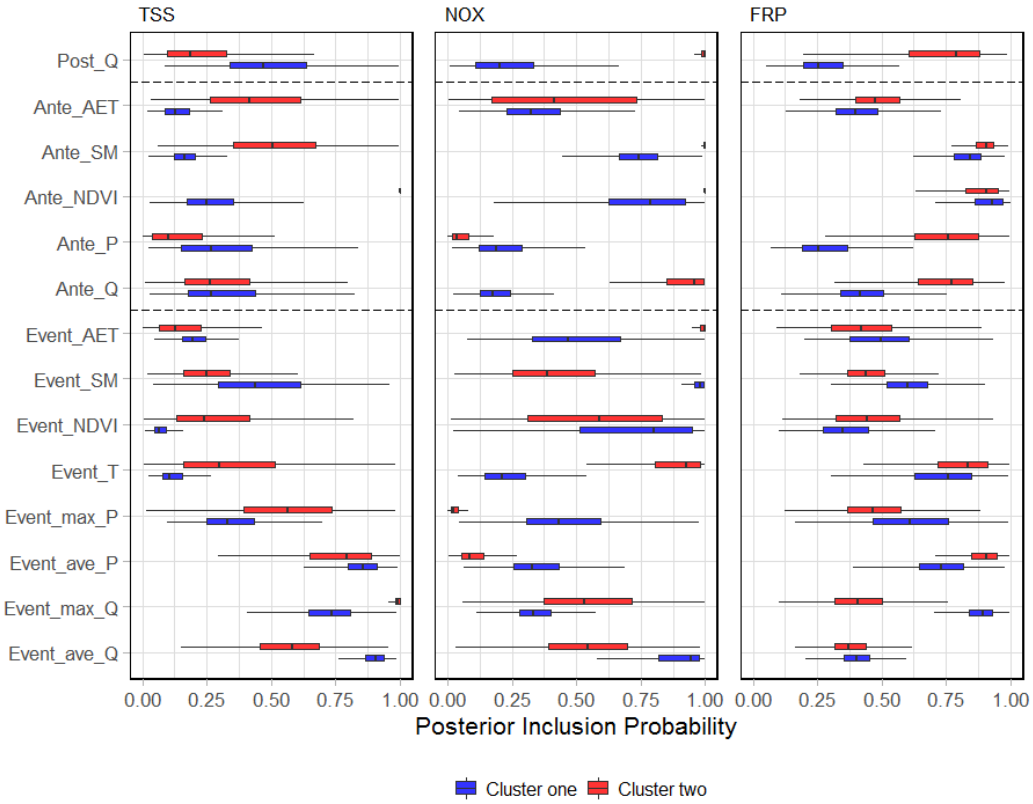

Figure 7: The comparisons of the distribution of posterior inclusion probabilities of the individual predictors derived from 1,000 subsampled BMA runs; the boxes are the interquartile ranges (IQR, 25th to 75th percentile), and the whiskers are the ranges between 1.5 IQR of the lower quartile and 1.5 IQR of the higher quartile; the vertical bar = median; blue = Cluster 1 ("wet"); red = Cluster 2 ("dry"); the definition of abbreviation of each predictor on y-axis are in Table 3.

3.2 Predictive performance

Moderate levels of temporal variability were explained by the BMA framework for the two independent clusters of sites (Figs.~~ure~~ 8, ~~Figures B8~~ B9 and ~~B9~~B10). At the cluster level, the NSE ranged from 0.04 (DOP) to 0.68 (EC) and from 0.34 (NH_4) to 0.64 (NO_X) for Clusters 1 and 2 (full model columns in Table ~~4~~C6, Appendix C), respectively. The comparison of the modelling performance (posterior median of BMA prediction) showed that the modelling framework performed better on the Cluster 2 sites than Cluster 1 (~~Figure~~ Fig. 8, red 50% prediction CI – Cluster 2), except for NH_4 and EC (not shown). This was reflected in a better match to the 1:1 line within the 90% prediction CI for Cluster two catchments. According to model performance criteria recommended by Moriasi et al. (2015), model performance is satisfactory (Table C7), especially for the Cluster 2 models. Generally, low NSE is acceptable for modelling nutrients and sediment compared to hydrology. It is also worth noting that, in contrast to the models developed here, most of the water quality models evaluated in Moriasi et al. (2015) are process-based models and focusing on individual catchments.

It is also worth noting that the prediction interval for EC (~~Figure~~ Fig. ~~B9~~ B10 [c]) was much wider than the rest of the constituents. Similar results were found in the site-level performance, with the average site-level NSE (~~Figure~~ Fig. ~~9~~B11) for Cluster 2 models typical higher than for Cluster 1. The site-specific performance varied across sites, with the largest variation in EC (NSE for the Cluster 2 result ranged from approximately 0.20 to 0.90). The modelling performance of DOP in the Cluster 1 sites was poor (NSE = 0.04); all candidate covariates had low predictive power, resulting in the poor mixing of chains of the inclusion variable I_n (i.e., posterior I_n was around 0.5). The model residuals were normally distributed (~~Figure~~ Fig. ~~B10~~B12) and there was no clear heteroscedasticity within the residuals (Fig~~ure~~s. ~~B11~~ B13 to ~~B19~~B21).

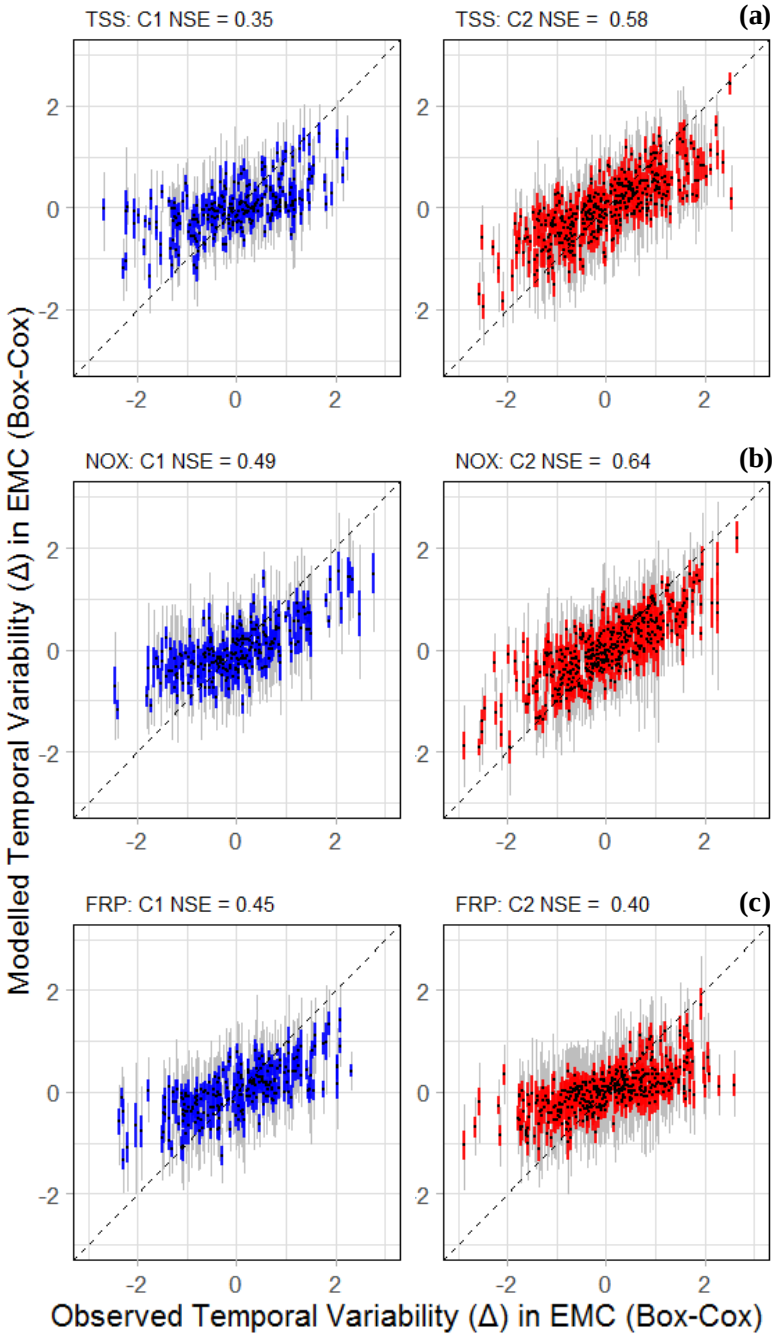

Figure 8: Performance of the BMA models of the temporal variability of three constituents across 32 sites, represented by prediction intervals from BMA and observed Box-Cox EMC across two clusters of sites for: (a) TSS; (b) NO_X; and (c) FRP. Each bar shows a single event and all events at all sites in the cluster are included. The NSE values were calculated based on median predictions. Black dots show prediction median; grey vertical lines show 95% CI; coloured vertical lines show 50% CI; blue is Cluster 1 ("wet"); red is Cluster 2 ("dry"); and dashed black lines are the 1:1 relationship.

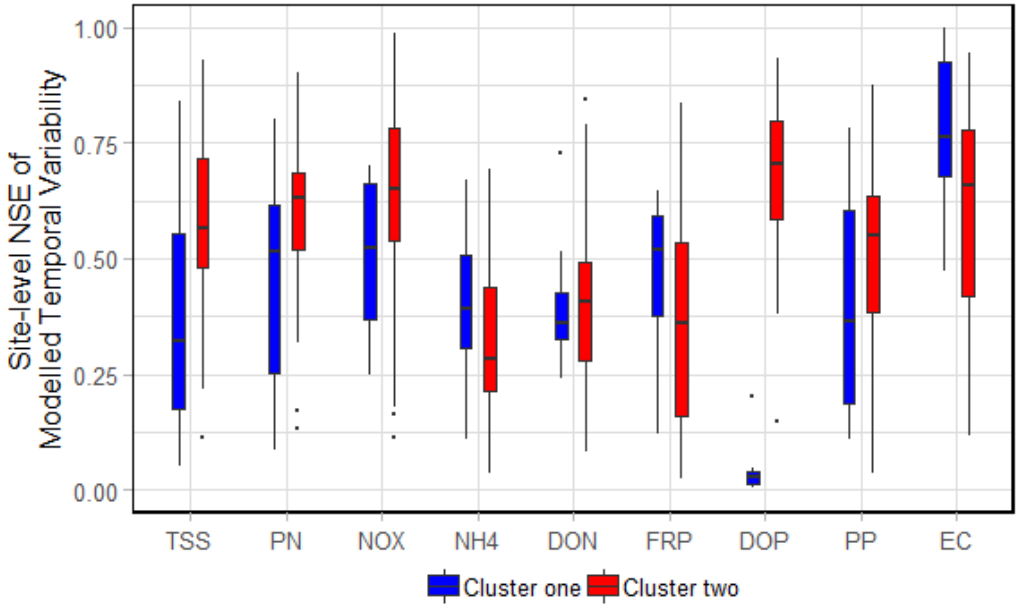

~~Figure 9: Distribution of site-level NSE for modelled the temporal variability of two clusters of sites. The interpretation of boxplot is the same as Figure 7. NSE values were calculated based on site-level predictions of event median EMC; blue is Cluster 1("wet"); and red is Cluster 2 ("dry") (i.e., each boxplot is comprised of respective number of sites in each cluster, one for each catchment).~~

Table ~~4~~ C6 (in Appendix C) compares the model performance using rainfall/runoff related predictors only and all candidate predictors (full model). A large increase in NSE was found for most dissolved nutrient species (e.g., NO_X, NH_4, DON, FRP and DOP) for the full model. Notably, for NH_4 in Cluster 1, factors other than rainfall and runoff explained almost all the variability that could be captured by the BMA.

~~Table 4: Comparison between BMA performance using rainfall/runoff predictors only and all candidate predictors (full models).~~

~~Constituent~~	~~NSE for Cluster 1 ("wet")~~			~~NSE for Cluster 2 ("dry")~~		
	~~Rainfall, runoff only~~	~~Full model~~	~~% change in NSE~~	~~Rainfall, runoff only~~	~~Full model~~	~~% change in NSE~~
~~TSS~~	~~0.32~~	~~0.35~~	~~11~~	~~0.42~~	~~0.58~~	~~38~~
~~PN~~	~~0.32~~	~~0.40~~	~~24~~	~~0.38~~	~~0.59~~	~~56~~
~~NO_X~~	~~0.23~~	~~0.49~~	~~113~~	~~0.32~~	~~0.64~~	~~101~~
~~NH_4~~	~~0.00~~	~~0.39~~	~~/~~	~~0.18~~	~~0.34~~	~~88~~
~~DON~~	~~0.20~~	~~0.37~~	~~84~~	~~0.20~~	~~0.43~~	~~117~~
~~FRP~~	~~0.27~~	~~0.45~~	~~68~~	~~0.26~~	~~0.40~~	~~56~~
~~DOP~~	~~0.00~~	~~0.04~~	~~/~~	~~0.22~~	~~0.62~~	~~181~~
~~PP~~	~~0.29~~	~~0.36~~	~~24~~	~~0.34~~	~~0.51~~	~~51~~
~~EC~~	~~0.41~~	~~0.68~~	~~66~~	~~0.39~~	~~0.54~~	~~39~~

4 Discussion

4.1 Factors influencing temporal variability in stream water quality

4.1.1 Runoff and rainfall

Our results demonstrated that runoff and rainfall were important factors in explaining the temporal dynamics of particulate pollutants (i.e., TSS, PN and PP) and dissolved species (e.g., NO_X, DOP and EC) in the GBR catchments. These results align with the findings of previous studies that have used these variables to understand changes in water quality over time (Beiter et al., 2020; McKergow et al., 2003; Schwarz et al., 2006).

Hydrologic and climatic variables (i.e., rainfall and runoff) showed distinct effects on different constituents, as well as different groups of catchments. The positive effect of event runoff and rainfall on sediment and particulate nutrients (i.e., PN, PP) revealed their underlying impacts on pollutant mobilisation and transport processes in catchments (Hirsch et al., 2010; Lintern et al., 2018b; Musolff et al., 2015). In contrast, there were negative effects of during-event runoff on NO_X (Cluster 1), DOP (Cluster 2) and EC (both clusters). For NO_X and EC, this was most likely caused by hydrological transport processes; these constituents tend to be transported to receiving rivers via subsurface flows (Kratz et al., 1997; McKergow et al., 2003). For events with relatively low surface runoff, higher NO_X and EC event concentrations could be expected in these catchments (Clow et al., 2000; Skoulikidis et al., 2006). In addition, for DOP, in-stream biogeochemical cycling was likely to have caused the negative effect of event runoff. The events with low runoff, coupled with high temperatures (positive effect of event temperature for DOP Cluster 2, ~~Figure~~ Fig. ~~B3~~ B4 [a]) may relate to increases in the rate of P releases from organic forms at higher temperatures (Verheyen et al., 2015).

Post-event runoff (*Post_Q*) showed effects on specific constituents (e.g., NOx, FRP and EC). Two alternative reasons might explain this. First, high post-event runoff may be an indicator of large baseflow contribution during the events (Cuomo et al., 2016). Therefore, as discussed in the above paragraph, constituents that can be transported through subsurface flows tend to be influenced by amount of runoff after event. Alternatively, it was significantly and positively correlated with other event characteristics and catchment biophysical conditions (e.g., vegetation cover, ~~Figure~~ Fig. ~~B1~~B2). These inter-correlated factors together could have influenced pollutant source, mobilisation and delivery (see discussions below) (Granger et al., 2010; Lintern et al., 2018a).

4.1.2 Vegetation cover

Vegetation cover was another driving factor that was found to have influenced water quality dynamics; antecedent NDVI (*Ante_NDVI*) was included in the plausible models more frequently than event NDVI. The negative effect of antecedent NDVI on particulate and dissolved nutrients (except for DOP) was in line with previous studies that have found that NDVI

was negatively correlated with these constituent concentrations in streams (Griffith et al., 2002; Masocha et al., 2017). An explanation for these results could be that high vegetation groundcover tended to stabilise the surface soil and reduce sediment losses by erosion (Meyer et al., 1997; Singh et al., 2008). In addition, vegetation nutrient assimilation and retention processes consumed nutrients in sediment and waterbodies, and these processes peaked in spring and early summer, typically before the wet season in the GBR catchments (Tabacchi et al., 2000; Vymazal, 2007).

The effect of antecedent NDVI varied among groups of constituents in Clusters 1 and 2. Specifically, it was a key predictor for NO_X, NH_4 and FRP for Cluster one, and almost all constituents for Cluster 2. This can be explained by the contrasting landscapes and climate of these two regions (Liu et al., 2018). In the dense, vegetation-covered catchments in Cluster 1 (i.e., the sites in the Wet Tropics), dissolved inorganic nutrient losses were likely due to more fertile soils (e.g., application of fertiliser on sugarcane) during the growing season (McKergow et al., 2005a). Furthermore, denser natural vegetation cover (e.g., riparian vegetation and forest) could increase plant uptake and assimilation of dissolved nutrients compared to the sparse vegetation cover in the Dry Tropics (Cluster 2) region. Conversely, among Cluster 2 sites, vegetation coverage showed clear seasonal variation, which was linked closely to the seasonality in rainfall and grazing activity. Sediments and particulate pollutants were likely to be mobilized in grazed catchments (high rate of soil erosion) and delivered to streams via surface runoff (Neil et al., 2002; Turner et al., 2012). More importantly, high vegetation cover tended to mitigate mobilisation of pollutants, through stabilising the surface soil and such that reduces sediment losses from erosion (Meyer et al., 1997; Singh et al., 2008).

4.1.3 Soil moisture and evapotranspiration

The results showed that soil moisture (SM) and actual evapotranspiration (AET) had a high impact on different constituents, particularly in the Cluster 2 catchments (e.g., antecedent soil moisture [DON and EC], antecedent AET [TSS and EC]). These two variables were inter-correlated and affect the hydrological cycle and vegetation cover (Correll, 1996). The results indicated that antecedent soil moisture had a negative effect on PN, NO_X, NH_4, DON, DOP and FRP. On one hand, this was expected as antecedent soil moisture was positively correlated with vegetation cover, and high soil moisture tends to reduce soil erosion and increase plant nutrient uptake. It may also be that soil water content affected soil microbial activity, influencing the biogeochemical processes in catchments, such as denitrification (Doran et al., 1988; Weier et al., 1993). The rate of denitrification was also enhanced under anoxic conditions, when soil moisture was high (Zhu et al., 2018a). On the other hand, higher soil water can be associated with increased shallow subsurface flow and leaching of some constituents such as NO_X (Zhu et al., 2018b). This appears not to occur to a sufficient extent for it to over-ride other impacts of soil moisture.

4.1.4 Temperature

Our results suggested that average event temperature (*Event_T*) had a positive effect on NO_X, FRP, and DOP. This may be attributed to the strong negative cross-correlation between temperature and event runoff and antecedent vegetation condition

(~~Figure~~ Fig. ~~B1~~B2). Rainfall during a warmer period might have been associated with less event runoff, resulting in higher event mean concentrations (Sect. 4.1.1). The effect of event temperature can be also attributed to the fact that the higher temperatures could lead to more recent mineralisation of nutrients, increasing readily transportable dissolved nutrient sources (Liu et al., 2017; Wang et al., 2020). Temperature is one controlling factor that affects pollution transformation (Barnard et al., 2005). For instance, temperature has a direct impact on the activity of microorganisms, which affects the intensity of biological processes such as denitrification (Wakelin et al., 2011). In addition, higher event temperature might be associated with higher pre-event temperature, resulting in poor groundcover, potentially lowering the dissolved nutrients losses through plant assimilation/uptake (Sect. 4.1.2~~.0~~) (Muro et al., 2018).

4.2 Predicting temporal variations in water quality

The Bayesian modelling framework in this study provided a useful tool to assess in-stream water quality dynamics. The models were able to explain more temporal variation in NO_X and EC than in other constituents. This is related to the sources and delivery processes of these two constituents. Anthropogenic inputs (e.g., agriculture) for NO_X, and large stores in groundwater together with limited geochemical transformation for EC (salts) suggested that temporal changes in event concentration could be well-captured by the changes in catchment hydroclimatic and vegetation conditions. In addition, NO_X and EC tend to be transported in subsurface flow pathways. The dynamics of catchment soil wetness and vegetation cover have been previously linked to hydrological interactions between surface and subsurface flows (Ursino et al., 2004). The incorporation of soil moisture and vegetation cover into the Bayesian modelling framework more readily allowed the description of the main ecohydrological processes of these two constituents.

In contrast, model performance for DOP was poor in Cluster 1 catchments, which can be explained by two reasons. First, in the Wet Tropics catchments, DOP concentrations were generally stable, regardless of changes in flow, which can be explained by chemical exchange processes between water and sediment in stream (White et al., 1998). This means that the variability in DOP cannot be captured by the environmental variables considered here. Second, the poor performance might be attributed to the data set having fewer observations of DOP EMCs among Cluster 1 sites. There were only 66 observations, compared to the next lowest number of 167 (EC) among other constituents in the Cluster 1 catchments, which may not be sufficient to fully inform the model. This small sample size could have led to outcomes of: 1) poor mixing of MCMC chains for inclusion variables (~~Figure~~ Fig. ~~B7~~ B8 [a]), where no predictors showed predictive power; and 2) the BMA failed to identify the plausible models, since none of the candidate models had enough predictive power to fit the data well (Guthke, 2017; Höge et al., 2019). Continuous DOP monitoring would be required to achieve a better understanding of the factors driving temporal variation in this constituent. Therefore, we did not infer any conclusions from the modelling results of DOP in Cluster 1 due to the poor modelling performance.

The modelling performance in this study is generally higher than our previous studies (i.e., Guo et al. (2019) and Guo et al. (2020)). This improved performance can be attributed to:

1) difference in water quality monitoring data

Rivers in Queensland are more event dominated, thus we used event-based water quality data, compared to our previous studies which used monthly water quality data in Victoria. The uncertainty in event-based water quality samples have less impact on modelling performance because we considered the variability in streamflow when developing EMCs in this study (Chen et al., 2017; Lessels et al., 2015; Letcher et al., 2002).

2) difference in modelling methods

Here, we used a model averaging approach that considered model predictions from multiple candidate models, rather than a single-model approach that was used our previous studies (Guo et al., 2020; Guo et al., 2019). This approach is a more robust approach to providing predictions because the predictions consider the model selection uncertainty (Höge et al., 2019; Raftery et al., 1997).

Statistical modelling in hydrology or water quality is affected by uncertainty, only some of which can be characterised within any particular modelling framework (Kavetski et al., 2006; Mantovan et al., 2006; Renard et al., 2010). The Bayesian modelling framework used in this study incorporated the uncertainties in model selection (between-model), observations and model parameters (within-model) directly into the model predictions (Steel, 2019). This is a more comprehensive characterisation than in studies where model structures are assumed *a priori*. Reporting of predictive uncertainty of temporal variations in water quality also provided valuable information on the confidence in the averaged predictions. In addition, as discussed in Sect. 2.3, due to strong practical and conceptual reasons, our modelling framework was applied to two clusters of sites separately. However, this method can be used anywhere, e.g., a single modelling framework for all sites. Thus, we are not making claims that there are always variables that will be important in such catchments. Our method is universal, but our results are not.

Nevertheless, limitations remain in the BMA approach which are important to understand. For example, for EC, there was a larger predictive uncertainty and larger uncertainty in posterior inclusion probability for each predictor from the robustness assessment than estimated in the fit to the complete data set. One limitation of BMA is that the posterior model probability could be sensitive to the specification of the parameter prior distribution (Fernandez et al., 2001). Specifying more informative priors on model parameters (i.e., inclusion variable I_n) would have the effect of restricting the set of candidate models (Rockey et al., 2016). Indeed, several studies have compared different predictive performances of different prior specification of BMA coefficients and found that the choice of prior matters (Bayarri et al., 2012; Liang et al., 2008). Future investigation of the sensitivity of prior distributions for BMA coefficients might achieve a reduction in predictive uncertainty and instability in posterior inclusion probabilities.

4.3 Management implications

The identification of key drivers of temporal variation in water quality can inform catchment water quality management. The results of this study showed that the effects of hydro-climatic drivers (e.g., rainfall and runoff) and vegetation cover varied among constituents and regions. This may allow funding bodies, such as government, regional natural resource management groups, to identify regions where land management and restoration would have a greater effect on mitigating

sediments and nutrients export. The results suggested that, compared to wet catchments, maintaining vegetation ground cover in large dry grazed catchments (e.g., the Burdekin and Fitzroy catchments in Cluster 2) before the wet seasons could be an effective way of reducing sediment losses via erosion processes. These results are consistent with current, improved land management practices across the GBR catchments (Brodie et al., 2012; Government, 2017). Management measures (e.g., establishment of wetlands, re-vegetation/rehabilitation of gully and stabilisation of river banks) can reduce sediment losses from hillslope and gully erosions (Koci et al., 2020; Sherriff et al., 2016). In addition, catchment-specific management that accounts for temporal variation in catchment hydrological connectivity is required for the control of dissolved nutrients. Dominant flow pathways for dissolved nutrients can vary spatially and temporally. For example, subsurface flow in the Wet Tropics region have tended to transmit more dissolved nutrient, because prolonged wet conditions lead to this region that is more likely to be connected via lateral subsurface flow (Geng et al., 2017). The enhanced mobilisation of leached dissolved nutrients from intensive cropping (e.g., sugarcane) from perched groundwater should be targeted in these catchments (Melland et al., 2012). Management practices, such as conservation tillage, and adaptation of '4R'concept (right source, right rate, right time, right place) for fertiliser application may help to minimise dissolved nitrogen losses (Lintern et al., 2020; Snyder, 2017).

5. Conclusions

This study provides a data-driven understanding of key drivers influencing the temporal variation in water quality. A hierarchical Bayesian model averaging framework was used to identify the key environmental drivers and predict the water quality dynamics at multiple catchments. Results showed that the temporal dynamics of water quality can be predicted well using models considering the combined effects of hydroclimate and vegetation groundcover. The effects of key hydro-climatic and vegetation conditions varied among different constituents, and across regions. This study reinforces the importance of vegetation cover management as one key management response, especially for large grazed catchments. Future investigation could involve the development of a spatio-temporal modelling framework to fully capture the water quality dynamics. More importantly, it has continued to be challenging to prioritise management practices and evaluate the effectiveness of the improved management interventions. Consequently, with more land management surveys and continuous water quality monitoring data available, an extended temporal or spatio-temporal modelling framework could potentially be used to assess if the success of the restoration measures.

Data availability

Water quality data that supported this study was available upon request from the Great Barrier Reef Catchment Loads Monitoring Program (GBREvents@dsiti.qld.gov.au). Sources of explanatory variables were listed in Table 2.

Author contribution

All authors contributed to the design of the research. SL carried out data collation, performed the simulations and prepared the manuscript with contributions from all co-authors. All authors contributed to the interpretation of the results and provided feedback.

Competing interests

The authors declare that they have no conflict of interest.

Acknowledgements

This study was supported by the Australian Research Council (LP140100495), the Environment Protection Authority Victoria, the Victorian Department of Environment, Land, Water and Planning, Bureau of Meteorology and Queensland Department of Natural Resources, Mines and Energy. The author would like to acknowledge the efforts of the Queensland Department of Environment and Science who provided the water quality monitoring data. The authors would also like to offer sincere gratitude to Ms. Jie Jian for her assistance in geospatial database compilation. Dr. Paul Leahy, Mr. Malcolm Watson, Dr. Ulrike Bende-Michl, Mr. Paul Wilson, and Ms. Belinda Thompson all of whom provided valuable advice in the preparation of this manuscript.

References

Abbaspour, Karim C, Rouholahnejad, Elham, Vaghefi, SRINIVASANB, Srinivasan, Raghavan, Yang, Hong, & Kløve, Bjørn. (2015). A continental-scale hydrology and water quality model for Europe: Calibration and uncertainty of a high-resolution large-scale SWAT model. *Journal of Hydrology, 524*, 733-752.

Abbott, MB, Bathurst, JC, Cunge, JA, O'connell, PE, & Rasmussen, J. (1986). An introduction to the European Hydrological System—Systeme Hydrologique Europeen,"SHE", 2: Structure of a physically-based, distributed modelling system. *Journal of Hydrology, 87*(1), 61-77.

Arnold, Jeffrey G, & Fohrer, Nicola. (2005). SWAT2000: current capabilities and research opportunities in applied watershed modelling. *Hydrological Processes, 19*(3), 563-572.

Atkinson, Anthony B. (2020). The box-cox transformation: Review and extensions. *Statistical science*.

Barnard, Romain, Leadley, Paul W, & Hungate, Bruce A. (2005). Global change, nitrification, and denitrification: a review. *Global biogeochemical cycles, 19*(1).

Bartley, Rebecca, Speirs, William J, Ellis, Tim W, & Waters, David K. (2012). A review of sediment and nutrient concentration data from Australia for use in catchment water quality models. *Marine pollution bulletin, 65*(4-9), 101-116.

Bartley, Rebecca, Thompson, Chris, Croke, Jacky, Pietsch, Tim, Baker, Brett, Hughes, Kate, & Kinsey-Henderson, Anne. (2018). Insights into the history and timing of post-European land use disturbance on sedimentation rates in catchments draining to the Great Barrier Reef. *Marine pollution bulletin, 131*, 530-546.

Bayarri, Maria J, Berger, James O, Forte, Anabel, & García-Donato, G. (2012). Criteria for Bayesian model choice with application to variable selection. *The Annals of statistics, 40*(3), 1550-1577.

Beiter, D., Weiler, M., & Blume, T. (2020). Characterising hillslope–stream connectivity with a joint event analysis of stream and groundwater levels. *Hydrol. Earth Syst. Sci., 24*(12), 5713-5744. doi: 10.5194/hess-24-5713-2020

Bieger, Katrin, Hörmann, Georg, & Fohrer, Nicola. (2014). Simulation of streamflow and sediment with the soil and water assessment tool in a data scarce catchment in the three Gorges region, China. *Journal of Environmental Quality, 43*(1), 37-45.

Box, George EP, & Cox, David R. (1964). An analysis of transformations. *Journal of the Royal Statistical Society: Series B (Methodological), 26*(2), 211-243.

Brevik, Eric C, Fenton, Thomas E, & Lazari, Andreas. (2006). Soil electrical conductivity as a function of soil water content and implications for soil mapping. *Precision Agriculture, 7*(6), 393-404.

Brodie, Jon Edward, Kroon, FJ, Schaffelke, Britta, Wolanski, EC, Lewis, SE, Devlin, MJ, Bohnet, IC, Bainbridge, ZT, Waterhouse, Jane, & Davis, AM. (2012). Terrestrial pollutant runoff to the Great Barrier Reef: an update of issues, priorities and management responses. *Marine pollution bulletin, 65*(4), 81-100.

Bureau of Meteorology. (2012). Geofabric V2. Retrieved 02/09/2016 ftp://ftp.bom.gov.au/anon/home/geofabric/

Castillo, Ismaël, Schmidt-Hieber, Johannes, & Van der Vaart, Aad. (2015). Bayesian linear regression with sparse priors. *Annals of Statistics, 43*(5), 1986-2018.

Chang, Fi-John, Tsai, Yu-Hsuan, Chen, Pin-An, Coynel, Alexandra, & Vachaud, Georges. (2015). Modeling water quality in an urban river using hydrological factors–Data driven approaches. *Journal of Environmental Management, 151*, 87-96.

Chen, Lei, Sun, Cheng, Wang, Guobo, Xie, Hui, & Shen, Zhenyao. (2017). Event-based nonpoint source pollution prediction in a scarce data catchment. *Journal of Hydrology, 552*, 13-27.

Clow, David W, & Sueker, Julie K. (2000). Relations between basin characteristics and stream water chemistry in alpine/subalpine basins in Rocky Mountain National Park, Colorado. *Water Resources Research, 36*(1), 49-61.

Cooke, Sandra E, Ahmed, Said M, & MacAlpine, Neil. (2000). *Introductory guide to surface water quality monitoring in agriculture*: Conservation and Development Branch, Alberta Agriculture, Food and Rural ….

Correll, DL. (1996). Buffer zones and water quality protection: general principles. *Buffer zones: Their processes and potential in water protection*, 7-20.

Cuomo, A, & Guida, D. (2016). Using hydro-chemograph analyses to reveal runoff generation processes in a Mediterranean catchment. *Hydrological Processes, 30*(24), 4462-4476.

Daoud, Jamal I. (2017). *Multicollinearity and regression analysis.* Paper presented at the Journal of Physics: Conference Series.

Davis, Aaron M, Pearson, Richard G, Brodie, Jon E, & Butler, Barry. (2017). Review and conceptual models of agricultural impacts and water quality in waterways of the Great Barrier Reef catchment area. *Marine and Freshwater Research, 68*(1), 1-19.

Day, Kenneth A, & McKeon, Gregory M. (2018). An index of summer rainfall for Queensland's grazing lands. *Journal of Applied Meteorology and Climatology, 57*(7), 1623-1641.

De Keersmaecker, Wanda, Lhermitte, Stef, Tits, Laurent, Honnay, Olivier, Somers, Ben, & Coppin, Pol. (2015). A model quantifying global vegetation resistance and resilience to short-term climate anomalies and their relationship with vegetation cover. *Global Ecology and Biogeography, 24*(5), 539-548.

de Mello, Kaline, Valente, Roberta Averna, Randhir, Timothy O, dos Santos, André Cordeiro Alves, & Vettorazzi, Carlos Alberto. (2018). Effects of land use and land cover on water quality of low-order streams in Southeastern Brazil: Watershed versus riparian zone. *Catena, 167*, 130-138.

Deletic, Ana B, & Maksimovic, CT. (1998). Evaluation of water quality factors in storm runoff from paved areas. *Journal of Environmental Engineering, 124*(9), 869-879.

Didan, K. (2015). MOD13A2 MODIS/Terra Vegetation Indices 16-Day L3 Global 1km SIN Grid V006, NASA EOSDIS LP DAAC (Publication no. 10.5067/MODIS/MOD13A2.006). https://earthdata.nasa.gov/

DNRME. (2018, 07/10/2016). Water Monitoring Information Portal. from https://water-monitoring.information.qld.gov.au/

Doran, JW, Mielke, LN, & Stamatiadis, S. (1988). *Microbial activity and N cycling as regulated by soil water-filled pore space.* Paper presented at the Proceedings of the 11th ISTRO Conference, Edinburgh, UK.

Fernandez, Carmen, Ley, Eduardo, & Steel, Mark FJ. (2001). Benchmark priors for Bayesian model averaging. *Journal of Econometrics, 100*(2), 381-427.

Filoso, Solange, Vallino, Joseph, Hopkinson, Charles, Rastetter, Edward, & Claessens, Luc. (2004). MODELING NITROGEN TRANSPORT IN THE IPSWICH RIVER BASIN, MASSACHUSETTS, USING A HYDROLOGICAL SIMULATION PROGRAM IN FORTRAN (HSPF) 1: Wiley Online Library.

Fox, John, Weisberg, Sanford, Adler, Daniel, Bates, Douglas, Baud-Bovy, Gabriel, Ellison, Steve, Firth, David, Friendly, Michael, Gorjanc, Gregor, & Graves, Spencer. (2012). Package 'car'. *Vienna: R Foundation for Statistical Computing*.

Francesconi, Wendy, Srinivasan, Raghavan, Pérez-Miñana, Elena, Willcock, Simon P, & Quintero, Marcela. (2016). Using the Soil and Water Assessment Tool (SWAT) to model ecosystem services: A systematic review. *Journal of Hydrology, 535*, 625-636.

Freckleton, Robert P. (2011). Dealing with collinearity in behavioural and ecological data: model averaging and the problems of measurement error. *Behavioral Ecology and Sociobiology, 65*(1), 91-101.

Frost, AJ, Ramchurn, A, & Smith, A. (2016). The Bureau's Operational AWRA Landscape (AWRA-L) Model. *Melbourne, Bureau of Meteorology, 47*.

Fu, Baihua, Merritt, Wendy S, Croke, Barry FW, Weber, Tony, & Jakeman, Anthony J. (2019). A review of catchment-scale water quality and erosion models and a synthesis of future prospects. *Environmental Modelling & Software, 114*, 75-97.

Garzon-Garcia, A, Wallace, Rohan, Huggins, Rae, Turner, Ryan DR, Smith, Rachael, Orr, David, Ferguson, Ben, Gardiner, Richard, Thomson, Belinda, & Warne, Michael. (2016). Total suspended solids, nutrient and pesticide loads (2013–2014) for rivers that discharge to the Great Barrier Reef.

Gelman, Andrew, Stern, Hal S, Carlin, John B, Dunson, David B, Vehtari, Aki, & Rubin, Donald B. (2013). *Bayesian data analysis*: Chapman and Hall/CRC.

Geng, Xiaolong, Heiss, James W, Michael, Holly A, & Boufadel, Michel C. (2017). Subsurface flow and moisture dynamics in response to swash motions: Effects of beach hydraulic conductivity and capillarity. *Water Resources Research, 53*(12), 10317-10335.

George, Edward I, & McCulloch, Robert E. (1993). Variable selection via Gibbs sampling. *Journal of the American Statistical Association, 88*(423), 881-889.

Geoscience Australia. (2008). GEODATA 9 second DEM and D8: digital elevation model version 3 and flow direction grid 2008. *Bioregion Assessment Source Dataset*.

Gilbert, M, & Brodie, JE. (2001). *Population and major land use in the Great Barrier Reef catchment area spatial and temporal trends*. Townsville.

Gorman, Daniel, Russell, Bayden D, & Connell, Sean D. (2009). Land-to-sea connectivity: linking human-derived terrestrial subsidies to subtidal habitat change on open rocky coasts. *Ecological Applications, 19*(5), 1114-1126.

Government, Queensland. (2017). *Reef 2050 Water Quality Improvement Plan - Management practices*. Brisbane.

Granger, SJ, Bol, R, Anthony, S, Owens, PN, White, SM, & Haygarth, PM. (2010). Towards a holistic classification of diffuse agricultural water pollution from intensively managed grasslands on heavy soils *Advances in Agronomy* (Vol. 105, pp. 83-115): Elsevier.

Griffith, Jerry A. (2002). Geographic techniques and recent applications of remote sensing to landscape-water quality studies. *Water, air, and soil pollution, 138*(1-4), 181-197.

Griffith, Jerry A, Martinko, Edward A, Whistler, Jerry L, & Price, Kevin P. (2002). Interrelationships among landscapes, NDVI, and stream water quality in the US Central Plains. *Ecological Applications, 12*(6), 1702-1718.

Guo, Danlu, Lintern, Anna, Webb, J Angus, Ryu, Dongryeol, Bende-Michl, Ulrike, Liu, Shuci, & Western, Andrew William. (2020). A data-based predictive model for spatiotemporal variability in stream water quality. *Hydrology and Earth System Sciences, 24*(2), 827-847.

Guo, Danlu, Lintern, Anna, Webb, J Angus, Ryu, Dongryeol, Liu, Shuci, Bende-Michl, Ulrike, Leahy, Paul, Wilson, Paul, & Western, AW. (2019). Key Factors Affecting Temporal Variability in Stream Water Quality. *Water Resources Research, 55*(1), 112-129.

Guthke, Anneli. (2017). Defensible model complexity: A call for data-based and goal-oriented model choice. *Groundwater, 55*(5), 646-650.

Harris, Graham P. (2001). Biogeochemistry of nitrogen and phosphorus in Australian catchments, rivers and estuaries: effects of land use and flow regulation and comparisons with global patterns. *Marine and Freshwater Research, 52*(1), 139-149.

Hem, John D. (1948). Fluctuations in concentration of dissolved solids of some southwestern streams. *Eos, Transactions American Geophysical Union, 29*(1), 80-84.

Hinne, Max, Gronau, Quentin F., van den Bergh, Don, & Wagenmakers, Eric-Jan. (2020). A Conceptual Introduction to Bayesian Model Averaging. *Advances in Methods and Practices in Psychological Science, 3*(2), 200-215. doi: 10.1177/2515245919898657

Hirsch, Robert M, Moyer, Douglas L, & Archfield, Stacey A. (2010). Weighted regressions on time, discharge, and season (WRTDS), with an application to Chesapeake Bay river inputs 1. *JAWRA Journal of the American Water Resources Association, 46*(5), 857-880.

Hoeting, Jennifer A, Raftery, Adrian E, & Madigan, David. (2002). Bayesian variable and transformation selection in linear regression. *Journal of Computational and Graphical Statistics, 11*(3), 485-507.

Höge, Marvin, Guthke, Anneli, & Nowak, Wolfgang. (2019). The hydrologist's guide to Bayesian model selection, averaging and combination. *Journal of Hydrology*.

Howarth, Robert W, Sharpley, Andrew, & Walker, Dan. (2002). Sources of nutrient pollution to coastal waters in the United States: Implications for achieving coastal water quality goals. *Estuaries, 25*(4), 656-676.

Jarihani, Ben, Sidle, Roy, Bartley, Rebecca, Roth, Christian, & Wilkinson, Scott. (2017). Characterisation of hydrological response to rainfall at multi spatio-temporal scales in savannas of semi-arid Australia. *Water, 9*(7), 540.

Jayakrishnan, RSRS, Srinivasan, R, Santhi, C, & Arnold, JG. (2005). Advances in the application of the SWAT model for water resources management. *Hydrological Processes: An International Journal, 19*(3), 749-762.

Kasiviswanathan, KS, & Sudheer, KP. (2013). Quantification of the predictive uncertainty of artificial neural network based river flow forecast models. *Stochastic Environmental Research and Risk Assessment, 27*(1), 137-146.

Kavetski, Dmitri, Kuczera, George, & Franks, Stewart W. (2006). Bayesian analysis of input uncertainty in hydrological modeling: 1. Theory. *Water Resources Research, 42*(3).

Khan, Urooj, Cook, Freeman J, Laugesen, Richard, Hasan, Mohammad M, Plastow, Kevin, Amirthanathan, Gnanathikkam E, Bari, Mohammed A, & Tuteja, Narendra K. (2020). Development of catchment water quality models within a realtime status and forecast system for the Great Barrier Reef. *Environmental Modelling & Software, 132*, 104790.

Koci, Jack, Sidle, Roy C, Jarihani, Ben, & Cashman, Matthew J. (2019). Linking hydrological connectivity to gully erosion in savanna rangelands tributary to the Great Barrier Reef using Structure-from-Motion photogrammetry. *Land Degradation & Development*.

Koci, Jack, Sidle, Roy C, Kinsey-Henderson, Anne E, Bartley, Rebecca, Wilkinson, Scott N, Hawdon, Aaron A, Jarihani, Ben, Roth, Christian H, & Hogarth, Luke. (2020). Effect of reduced grazing pressure on sediment and nutrient yields in savanna rangeland streams draining to the Great Barrier Reef. *Journal of Hydrology, 582*, 124520.

Kohavi, Ron. (1995). *A study of cross-validation and bootstrap for accuracy estimation and model selection.* Paper presented at the Ijcai.

Kratz, Timothy, Webster, Katherine, Bowser, Carl, Maguson, John, & Benson, Barbara. (1997). The influence of landscape position on lakes in northern Wisconsin. *Freshwater Biology, 37*(1), 209-217.

Kruschke, John. (2014). *Doing Bayesian data analysis: A tutorial with R, JAGS, and Stan*: Academic Press.

Kuhnert, Petra, Wang, You-Gan, Henderson, Brent, Stewart, Lachlan, & Wilkinson, Scott. (2009). Statistical methods for the estimation of pollutant loads from monitoring data. *Final Project Report. Report to the Marine and Tropical Sciences Research Facility, Reef and Rainforest Research Centre Limited, Cairns*.

Ladson, Anthony Richard, Brown, R, Neal, B, & Nathan, R. (2013). A standard approach to baseflow separation using the Lyne and Hollick filter. *Australasian Journal of Water Resources, 17*(1), 25-34.

Lam, QD, Schmalz, Britta, & Fohrer, N. (2010). Modelling point and diffuse source pollution of nitrate in a rural lowland catchment using the SWAT model. *Agricultural Water Management, 97*(2), 317-325.

Lessels, JS, & Bishop, TFA. (2015). A simulation based approach to quantify the difference between event-based and routine water quality monitoring schemes. *Journal of Hydrology: Regional Studies, 4*, 439-451.

Letcher, Rebecca A, Jakeman, Anthony J, Calfas, M, Linforth, S, Baginska, B, & Lawrence, I. (2002). A comparison of catchment water quality models and direct estimation techniques. *Environmental Modelling & Software, 17*(1), 77-85.

Liang, Feng, Paulo, Rui, Molina, German, Clyde, Merlise A, & Berger, Jim O. (2008). Mixtures of g priors for Bayesian variable selection. *Journal of the American Statistical Association, 103*(481), 410-423.

Lintern, A, Webb, JA, Ryu, D, Liu, S, Bende-Michl, U, Waters, D, Leahy, P, Wilson, P, & Western, AW. (2018a). Key factors influencing differences in stream water quality across space. *Wiley Interdisciplinary Reviews: Water, 5*(1), e1260.

Lintern, A, Webb, JA, Ryu, D, Liu, S, Waters, D, Leahy, P, Bende-Michl, U, & Western, AW. (2018b). What are the key catchment characteristics affecting spatial differences in riverine water quality? *Water Resources Research, 54*(10), 7252-7272.

Lintern, Anna, McPhillips, Lauren, Winfrey, Brandon, Duncan, Jonathan, & Grady, Caitlin. (2020). Best Management Practices for Diffuse Nutrient Pollution: Wicked Problems Across Urban and Agricultural Watersheds. *Environmental science & technology, 54*(15), 9159-9174.

Liu, S, Ryu, D, Webb, JA, Lintern, A, Waters, D, Guo, Danlu, & Western, AW. (2018). Characterisation of spatial variability in water quality in the Great Barrier Reef catchments using multivariate statistical analysis. *Marine pollution bulletin, 137*, 137-151. doi: https://doi.org/10.1016/j.marpolbul.2018.10.019

Liu, Yuan, Wang, Changhui, He, Nianpeng, Wen, Xuefa, Gao, Yang, Li, Shenggong, Niu, Shuli, Butterbach-Bahl, Klaus, Luo, Yiqi, & Yu, Guirui. (2017). A global synthesis of the rate and temperature sensitivity of soil nitrogen mineralization: latitudinal patterns and mechanisms. *Global change biology, 23*(1), 455-464.

Lloyd, CEM, Freer, JE, Johnes, PJ, & Collins, AL. (2016). Using hysteresis analysis of high-resolution water quality monitoring data, including uncertainty, to infer controls on nutrient and sediment transfer in catchments. *Science of the Total Environment, 543*, 388-404.

Ly, Kongmeng, Metternicht, Graciela, & Marshall, Lucy. (2019). Transboundary river catchment areas of developing countries: Potential and limitations of watershed models for the simulation of sediment and nutrient loads. A review. *Journal of Hydrology: Regional Studies, 24*, 100605.

Mainali, Janardan, Chang, Heejun, & Chun, Yongwan. (2019). A review of spatial statistical approaches to modeling water quality. *Progress in Physical Geography: Earth and Environment, 0*(0), 0309133319852003. doi: 10.1177/0309133319852003

Mantovan, Pietro, & Todini, Ezio. (2006). Hydrological forecasting uncertainty assessment: Incoherence of the GLUE methodology. *Journal of Hydrology, 330*(1-2), 368-381.

Masocha, Mhosisi, Murwira, Amon, Magadza, Christopher HD, Hirji, Rafik, & Dube, Timothy. (2017). Remote sensing of surface water quality in relation to catchment condition in Zimbabwe. *Physics and Chemistry of the Earth, Parts A/B/C, 100*, 13-18.

McCloskey, GL, Baheerathan, R, Dougall, C, Ellis, R, Bennett, FR, Waters, D, Darr, S, Fentie, B, Hateley, LR, & Askildsen, M. (2021). Modelled estimates of fine sediment and particulate nutrients delivered from the Great Barrier Reef catchments. *Marine pollution bulletin, 165*, 112163.

McGrane, Scott J. (2016). Impacts of urbanisation on hydrological and water quality dynamics, and urban water management: a review. *Hydrological Sciences Journal, 61*(13), 2295-2311.

McKergow, Lucy A, Prosser, Ian P, Hughes, Andrew O, & Brodie, Jon. (2005a). Regional scale nutrient modelling: exports to the Great Barrier Reef world heritage area. *Marine pollution bulletin, 51*(1-4), 186-199.

McKergow, Lucy A, Prosser, Ian P, Hughes, Andrew O, & Brodie, Jon. (2005b). Sources of sediment to the Great Barrier Reef world heritage area. *Marine pollution bulletin, 51*(1), 200-211.

McKergow, Lucy A, Weaver, David M, Prosser, Ian P, Grayson, Rodger B, & Reed, Adrian EG. (2003). Before and after riparian management: sediment and nutrient exports from a small agricultural catchment, Western Australia. *Journal of Hydrology, 270*(3-4), 253-272.

Melland, AR, Mellander, P-E, Murphy, PNC, Wall, DP, Mechan, S, Shine, O, Shortle, G, & Jordan, Philip. (2012). Stream water quality in intensive cereal cropping catchments with regulated nutrient management. *Environmental Science & Policy, 24*, 58-70.

Merritt, Wendy S, Letcher, Rebecca A, & Jakeman, Anthony J. (2003). A review of erosion and sediment transport models. *Environmental Modelling & Software, 18*(8), 761-799.

Meyer, David L, Townsend, Edward C, & Thayer, Gordon W. (1997). Stabilization and erosion control value of oyster cultch for intertidal marsh. *Restoration Ecology, 5*(1), 93-99.

Moriasi, Daniel N, Gitau, Margaret W, Pai, Naresh, & Daggupati, Prasad. (2015). Hydrologic and water quality models: Performance measures and evaluation criteria. *Transactions of the ASABE, 58*(6), 1763-1785.

Muro, Javier, Strauch, Adrian, Heinemann, Sascha, Steinbach, Stefanie, Thonfeld, Frank, Waske, Björn, & Diekkrüger, Bernd. (2018). Land surface temperature trends as indicator of land use changes in wetlands. *International journal of applied earth observation and geoinformation, 70*, 62-71.

Musolff, Andreas, Schmidt, Christian, Selle, Benny, & Fleckenstein, Jan H. (2015). Catchment controls on solute export. *Advances in Water Resources, 86*, 133-146. doi: https://doi.org/10.1016/j.advwatres.2015.09.026

Nakagawa, Shinichi, & Freckleton, Robert P. (2011). Model averaging, missing data and multiple imputation: a case study for behavioural ecology. *Behavioral Ecology and Sociobiology, 65*(1), 103-116.

Nash, J Eamonn, & Sutcliffe, Jonh V. (1970). River flow forecasting through conceptual models part I—A discussion of principles. *Journal of Hydrology, 10*(3), 282-290.

Neil, David T, Orpin, Alan R, Ridd, Peter V, & Yu, Bofu. (2002). Sediment yield and impacts from river catchments to the Great Barrier Reef lagoon: a review. *Marine and Freshwater Research, 53*(4), 733-752.

O'Hara, Robert B, & Sillanpää, Mikko J. (2009). A review of Bayesian variable selection methods: what, how and which. *Bayesian analysis, 4*(1), 85-117.

Orr, D., Turner, R.D.R., Huggins, R., Vardy, S., & J., Warne. M. St. (2014). *Wet Tropics water quality statistics for high and base flow conditions.* Brisbane.

Paliwal, Ritu, Sharma, Prateek, & Kansal, Arun. (2007). Water quality modelling of the river Yamuna (India) using QUAL2E-UNCAS. *Journal of Environmental Management, 83*(2), 131-144.

Peel, Murray C, Finlayson, Brian L, & McMahon, Thomas A. (2007). Updated world map of the Köppen-Geiger climate classification. *Hydrology and Earth System Sciences Discussions, 4*(2), 439-473. doi: https://doi.org/10.5194/hess-11-1633-2007

Pérez-Gutiérrez, Juan D, Paz, Joel O, & Tagert, Mary Love M. (2017). Seasonal water quality changes in on-farm water storage systems in a south-central US agricultural watershed. *Agricultural Water Management, 187*, 131-139.

Pilgrim, Ed, Institution of Engineers, Australia, Pilgrim, DH, & Canterford, RP. (1987). *Australian rainfall and runoff*: Institution of Engineers, Australia.

Plummer, Martyn. (2013a). JAGS: Just another Gibbs sampler, version 3.4. 0. *URL http://mcmc-jags. sourceforge. net*.

Plummer, Martyn. (2013b). rjags: Bayesian graphical models using MCMC. *R package version, 3*(10).

Posch, Konstantin, Arbeiter, Maximilian, & Pilz, Juergen. (2020). A novel Bayesian approach for variable selection in linear regression models. *Computational Statistics & Data Analysis, 144*, 106881.

Qi, Junyu, Li, Sheng, Bourque, Charles PA, Xing, Zisheng, & Fan-Rui, Meng. (2018). Developing a decision support tool for assessing land use change and BMPs in ungauged watersheds based on decision rules provided by SWAT simulation. *Hydrology and Earth System Sciences, 22*(7), 3789-3806.

R Core Team. (2013). R: A language and environment for statistical computing.

Raftery, Adrian E, Madigan, David, & Hoeting, Jennifer A. (1997). Bayesian model averaging for linear regression models. *Journal of the American Statistical Association, 92*(437), 179-191.

Raupach, MR, Briggs, PR, Haverd, V, King, EA, Paget, M, & Trudinger, CM. (2009). Australian water availability project (AWAP): CSIRO marine and atmospheric research component: final report for phase 3. *Melbourne: Centre for Australian weather and climate research (bureau of meteorology and CSIRO), 67*.

Ren, Wenwei, Zhong, Yang, Meligrana, John, Anderson, Bruce, Watt, W Edgar, Chen, Jiakuan, & Leung, Hok-Lin. (2003). Urbanization, land use, and water quality in Shanghai: 1947–1996. *Environment international, 29*(5), 649-659.

Renard, Benjamin, Kavetski, Dmitri, Kuczera, George, Thyer, Mark, & Franks, Stewart W. (2010). Understanding predictive uncertainty in hydrologic modeling: The challenge of identifying input and structural errors. *Water Resources Research, 46*(5).

Richards, R Peter, & Baker, David B. (1993). Trends in nutrient and suspended sediment concentrations in Lake Erie tributaries, 1975–1990. *Journal of Great Lakes Research, 19*(2), 200-211.

Rockey, James, & Temple, Jonathan. (2016). Growth econometrics for agnostics and true believers. *European Economic Review, 81*, 86-102.

Rode, Michael, Arhonditsis, George, Balin, Daniela, Kebede, Tesfaye, Krysanova, Valentina, Van Griensven, Ann, & Van der Zee, Sjoerd EATM. (2010). New challenges in integrated water quality modelling. *Hydrological Processes, 24*(24), 3447-3461.

Schwarz, GE, Hoos, AB, Alexander, RB, & Smith, RA. (2006). The SPARROW surface water-quality model: theory, application and user documentation. *US geological survey techniques and methods report, book, 6*(10).

Sherriff, SC, Rowan, JS, Melland, AR, Jordan, P, Fenton, O, & O hUallachain, DO. (2015). Investigating suspended sediment dynamics in contrasting agricultural catchments using ex situ turbidity-based suspended sediment monitoring. *Hydrology and Earth System Sciences, 19*, 3349-3363.

Sherriff, Sophie C, Rowan, John S, Fenton, Owen, Jordan, Philip, Melland, Alice R, Mellander, Per-Erik, & Huallachain, Daire O. (2016). Storm event suspended sediment-discharge hysteresis and controls in agricultural watersheds: implications for watershed scale sediment management. *Environmental science & technology, 50*(4), 1769-1778.

Shi, Peng, Zhang, Yan, Li, Zhanbin, Li, Peng, & Xu, Guoce. (2017). Influence of land use and land cover patterns on seasonal water quality at multi-spatial scales. *Catena, 151*, 182-190.

Singh, Aditya, Jakubowski, Andrew R, Chidister, Ian, & Townsend, Philip A. (2013). A MODIS approach to predicting stream water quality in Wisconsin. *Remote Sensing of Environment, 128*, 74-86.

Singh, PK, Bhunya, PK, Mishra, SK, & Chaube, UC. (2008). A sediment graph model based on SCS-CN method. *Journal of Hydrology, 349*(1-2), 244-255.

Skoulikidis, N Th, Amaxidis, Y, Bertahas, I, Laschou, S, & Gritzalis, K. (2006). Analysis of factors driving stream water composition and synthesis of management tools—a case study on small/medium Greek catchments. *Science of the Total Environment, 362*(1-3), 205-241. doi: https://10.1016/j.scitotenv.2005.05.018

Snyder, Clifford S. (2017). Enhanced nitrogen fertiliser technologies support the '4R'concept to optimise crop production and minimise environmental losses. *Soil Research, 55*(6), 463-472.

Srivastav, RK, Sudheer, KP, & Chaubey, I. (2007). A simplified approach to quantifying predictive and parametric uncertainty in artificial neural network hydrologic models. *Water Resources Research, 43*(10).

Steel, Mark FJ. (2019). Model averaging and its use in economics. *arXiv preprint arXiv:1709.08221*.

Tabacchi, Eric, Lambs, Luc, Guilloy, Helene, Planty-Tabacchi, Anne-Marie, Muller, Etienne, & Decamps, Henri. (2000). Impacts of riparian vegetation on hydrological processes. *Hydrological Processes, 14*(16-17), 2959-2976.

Tang, Weigang, & Carey, Sean K. (2017). HydRun: A MATLAB toolbox for rainfall–runoff analysis. *Hydrological Processes, 31*(15), 2670-2682.

Thompson, SE, Basu, NB, Lascurain, J, Aubeneau, A, & Rao, PSC. (2011). Relative dominance of hydrologic versus biogeochemical factors on solute export across impact gradients. *Water Resources Research, 47*(10).

Turner, R, Huggins, R, Wallace, R, Smith, R, Vardy, S, & Warne, M St J. (2012). Sediment, Nutrient and Pesticide Loads: Great Barrier Reef Catchment Loads Monitoring 2009-2010, Department of Science. *Information Technology, Innovation and the Arts, Brisbane*, 53.

Tweed, Sarah O, Leblanc, Marc, Webb, John A, & Lubczynski, Maciek W. (2007). Remote sensing and GIS for mapping groundwater recharge and discharge areas in salinity prone catchments, southeastern Australia. *Hydrogeology journal, 15*(1), 75-96.

Ursino, Nadia, Silvestri, Sonia, & Marani, Marco. (2004). Subsurface flow and vegetation patterns in tidal environments. *Water Resources Research, 40*(5).

Ustaoğlu, Fikret, Tepe, Yalçın, & Taş, Beyhan. (2020). Assessment of stream quality and health risk in a subtropical Turkey river system: A combined approach using statistical analysis and water quality index. *Ecological Indicators, 113*, 105815.

Verheyen, Dries, Van Gaelen, Nele, Ronchi, Benedicta, Batelaan, Okke, Struyf, Eric, Govers, Gerard, Merckx, Roel, & Diels, Jan. (2015). Dissolved phosphorus transport from soil to surface water in catchments with different land use. *Ambio, 44*(2), 228-240.

Vymazal, Jan. (2007). Removal of nutrients in various types of constructed wetlands. *Science of the Total Environment, 380*(1-3), 48-65.

Wade, Andrew J, Durand, Patrick, Beaujouan, Véronique, Wessel, Wim W, Raat, Klaasjan J, Whitehead, Paul G, Butterfield, Dan, Rankinen, Katri, & Lepisto, Ahti. (2002). A nitrogen model for European catchments: INCA, new model structure and equations. *Hydrology and Earth System Sciences Discussions, 6*(3), 559-582.

Wakelin, Steven A, Nelson, Paul N, Armour, John D, Rasiah, Velupillai, & Colloff, Matthew J. (2011). Bacterial community structure and denitrifier (nir-gene) abundance in soil water and groundwater beneath agricultural land in tropical North Queensland, Australia. *Soil Research, 49*(1), 65-76.

Walker, Jeffrey A. (2019). Model-averaged regression coefficients have a straightforward interpretation using causal conditioning. *BioRxiv*, 133785. doi: 10.1101/133785

Walling, DE. (1984). Dissolved loads and their measurement. *Erosion and Sediment Yield: Some Methods of Measurement and Modelling. Geo Books, Regency House Norwich(England). 1984. p 111-177, 18 fig, 10 tab, 104 ref.*

Wan, Yongshan, Qian, Yun, Migliaccio, Kati White, Li, Yuncong, & Conrad, Cecilia. (2014). Linking spatial variations in water quality with water and land management using multivariate techniques. *Journal of Environmental Quality, 43*(2), 599-610.

Wang, Ai, Yang, Dawen, & Tang, Lihua. (2020). Spatiotemporal variation in nitrogen loads and their impacts on river water quality in the upper Yangtze River basin. *Journal of Hydrology, 590*, 125487.

Wang, QJ, Schepen, Andrew, & Robertson, David E. (2012). Merging seasonal rainfall forecasts from multiple statistical models through Bayesian model averaging. *Journal of Climate, 25*(16), 5524-5537.

Waters, D, & Packett, R. (2007). *Sediment and nutrient generation rates for Queensland rural catchments-an event monitoring program to improve water quality modelling.* Paper presented at the Proceedings of the 5th Australian Stream Management Conference. Australian rivers: making a difference. Charles Sturt University, Thurgoona, New South Wales.

Webb, Angus, & King, Elise L. (2009). A Bayesian hierarchical trend analysis finds strong evidence for large-scale temporal declines in stream ecological condition around Melbourne, Australia. *Ecography, 32*(2), 215-225.

Weier, KL, Doran, JW, Power, JF, & Walters, DT. (1993). Denitrification and the dinitrogen/nitrous oxide ratio as affected by soil water, available carbon, and nitrate. *Soil Science Society of America Journal, 57*(1), 66-72.

Wellen, Christopher, Kamran-Disfani, Ahmad-Reza, & Arhonditsis, George B. (2015). Evaluation of the current state of distributed watershed nutrient water quality modeling. *Environmental science & technology, 49*(6), 3278-3290.

White, RE, Edis, RB, Bramley, RGV, & Wood, AW. (1998). Environmentally sound phosphorus management for sugarcane soils: final report on SRDC Project no CSS3S.

Wintle, Brendan A, McCarthy, Michel A, Volinsky, Chris T, & Kavanagh, Rodney P. (2003). The use of Bayesian model averaging to better represent uncertainty in ecological models. *Conservation biology, 17*(6), 1579-1590.

Zhang, Junlong, Zhang, Yongqiang, Song, Jinxi, & Cheng, Lei. (2017). Evaluating relative merits of four baseflow separation methods in Eastern Australia. *Journal of Hydrology, 549*, 252-263.

Zhang, Yuan, Guo, Fen, Meng, Wei, & Wang, Xi-Qin. (2009). Water quality assessment and source identification of Daliao river basin using multivariate statistical methods. *Environmental monitoring and assessment, 152*(1-4), 105.

Zhu, Guibing, Wang, Shanyun, Wang, Cheng, Zhou, Liguang, Zhao, Siyan, Li, Yixiao, Li, Fangbai, Jetten, Mike SM, Lu, Yonglong, & Schwark, Lorenz. (2018a). Resuscitation of anammox bacteria after> 10,000 years of dormancy. *The ISME journal*.

Zhu, Qing, Castellano, Michael J, & Yang, Guishan. (2018b). Coupling soil water processes and nitrogen cycle across spatial scales: Potentials, bottlenecks and solutions. *Earth-Science Reviews*.

Appendix A - Text

Hierarchical prior specification and Bayesian inference of key drivers

Bayesian inference required specification of prior distributions for each model parameter. A minimally-informative uniform prior (denote as $U(\cdot)$) between 0 and 10 was assigned to the global standard deviation (σ, Eq. A1) (Gelman, 2006). The prior of I_n assumes that each indicator comes from an independent Bernoulli distribution, with a probability of 0.5 (Eq. A2) (Raftery et al., 1997). This vague prior results in each model structure having an equal prior model probability.

$$\sigma \sim U(0,10) \quad \text{A1}$$

$$I_n \sim Bernoulli(0.5) \quad \text{A2}$$

We used a hierarchical conditional prior specification for predictor coefficients, allowing the site-specific parameter values that describe the effects of each temporal predictors ($\beta_{1,j}, \beta_{2,j}, \ldots, \beta_{n,j}$) to be exchangeable between sites (Liu et al., 2008; O'Hara and Sillanpää, 2009; Webb and King, 2009). The prior of $\beta_{n,j}$ was conditioned on I_n, resulting in a mixture distribution with 'slab and spike' prior, which was defined as follows,

$$\beta_{n,j} \left| I_n \right. \sim I_n N(0,\tau_n) + (1-I_n) N(0,\tau_{n,tune}) \quad \text{A3}$$

where $\beta_{n,j} \mid (I_n = 1)$ is the slab part of the mixture distribution. The $\beta_{n,j} \mid (I_n = 1)$ was estimated by including a higher-level distribution. The prior of $\beta_{n,j} \mid (I_n = 1)$ followed a normal distribution with random effect (Eq. A4), with the τ_n drawn from a common prior distribution, defined as a hyperparameter (i.e., uniform distribution between 0 to 20, Eq. A5) (Gelman, 2006; Kruschke, 2014).

$$\beta_{n,j} \left| (I_n = 1) \sim N(0,\tau_n) \right. \quad \text{A4}$$

$$\tau_n \sim U(0,20) \quad \text{A5}$$

For the spike component, a data-dependent prior was specified for $\beta_{n,j} \mid (I_n = 0)$, drawing from a *pseudo-prior* (Eq. A6), that is, *a priori* distribution with no effect on the posterior distribution, but facilitating the mixing of the Gibbs sampler.

$$\beta_{n,j} \left| (I_n = 0) \sim N(0,\tau_{n,tune}) \right. \quad \text{A6}$$

We estimated $\tau_{n,tune}$ from the standard deviations of the posterior of the $\beta_{n,j}$ in a global model structure (i.e., modelling structure using all predictors), as suggested by Carlin and Chib (1995) and Linden and Roloff (2015). The prior of $\beta_{n,j} \mid (I_n = 0)$ was near the posterior estimates to facilitate mixing in the MCMC (Hooten and Hobbs, 2015).

The posterior inclusion probability (PIP - $P(I_n = 1 \left| \boldsymbol{y} \right.)$, Eq. A7) of each predictor was used to compare the relative importance of individual predictors (i.e., how often the n^{th} predictor was 'in' the model).

$$P(I_n = 1 \left| \boldsymbol{y} \right.) = \frac{1}{T} \sum_{t=1}^{T} I(I_n^{(t)} = 1) \quad \text{A7}$$

where T is the total number of iterations of Markov chains. The different combination of I_n at each MCMC sampling represents a specific model structure. According to Bayes' theorem, the posterior model probability (PMP - $P(M_k \left| \boldsymbol{y} \right.)$) can be estimated as,

$$P(M_k \mid \boldsymbol{y}) = \frac{[\boldsymbol{y} \mid M_k]P(M_k)}{\sum_{x=1}^{L}[\boldsymbol{y} \mid M_x]P(M_x)} \quad \text{A8}$$

where L is the total number of possible models, and $P(M_k)$ is the prior probability of model M_k, among a group of models M_x, $x = 1, \ldots, X$. This posterior model probability can be obtained by assessing the frequency of a particular combination of I_n during the MCMC sampling.

Reference

Carlin, B. P. and Chib, S.: Bayesian model choice via Markov chain Monte Carlo methods, Journal of the Royal Statistical Society: Series B (Methodological), 57, 473-484, 1995.

Gelman, A.: Prior distributions for variance parameters in hierarchical models (comment on article by Browne and Draper), Bayesian analysis, 1, 515-534, 2006.

Hooten, M. B. and Hobbs, N. T.: A guide to Bayesian model selection for ecologists, Ecological Monographs, 85, 3-28, 2015.

Kruschke, J.: Doing Bayesian data analysis: A tutorial with R, JAGS, and Stan, Academic Press, 2014.

Linden, D. W. and Roloff, G. J.: Improving inferences from short-term ecological studies with Bayesian hierarchical modeling: white-headed woodpeckers in managed forests, Ecology and evolution, 5, 3378-3388, 2015.

Liu, Y., Guo, H., Mao, G., and Yang, P.: A bayesian hierarchical model for urban air quality prediction under uncertainty, Atmospheric Environment, 42, 8464-8469, 2008.

O'Hara, R. B. and Sillanpää, M. J.: A review of Bayesian variable selection methods: what, how and which, Bayesian analysis, 4, 85-117, 2009.

Raftery, A. E., Madigan, D., and Hoeting, J. A.: Bayesian model averaging for linear regression models, Journal of the American Statistical Association, 92, 179-191, 1997.

Webb, A. and King, E. L.: A Bayesian hierarchical trend analysis finds strong evidence for large-scale temporal declines in stream ecological condition around Melbourne, Australia, Ecography, 32, 215-225, 2009.

Appendix B - Figure

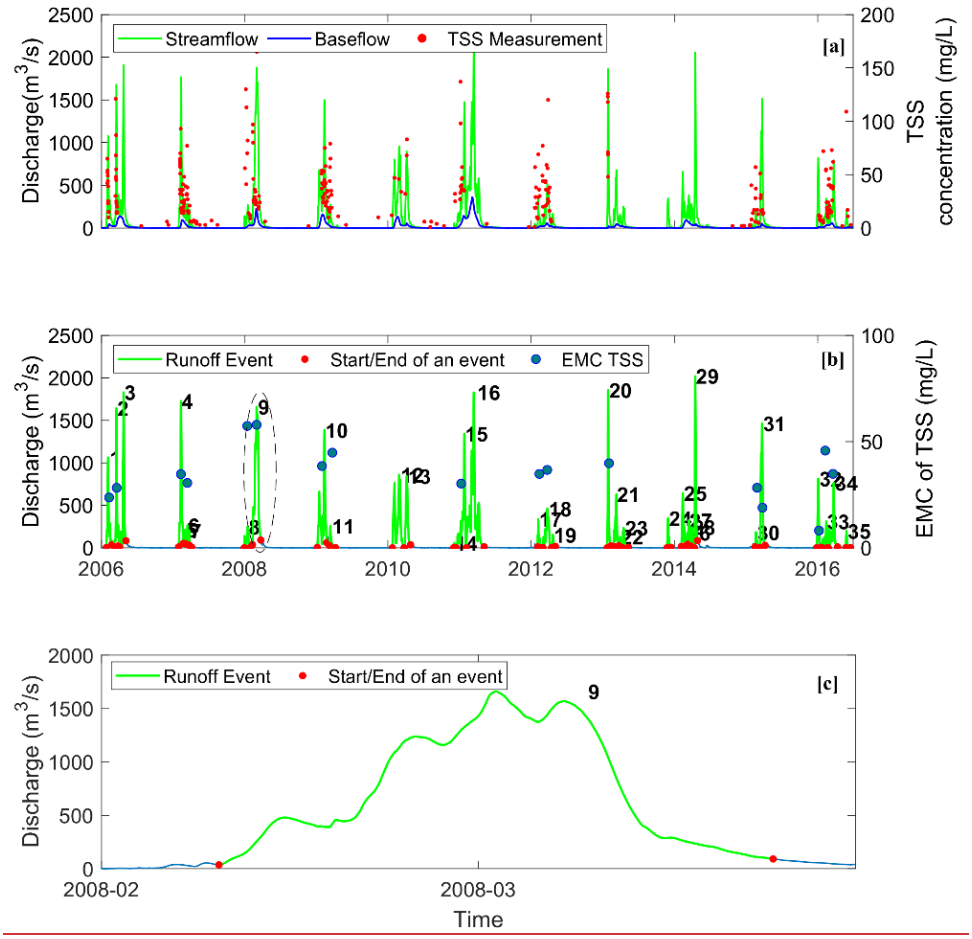

Figure B1: Delineation of runoff events and estimation of EMCs, based on the hydrograph for 105107A Normanby River at Kalpowar Crossing in the GBR catchments: [a] baseflow separation from continuous streamflow observations; [b] event identification and development of EMC, and 35 runoff events are identified with red dots representing either the start or end of a runoff event; and [c] A zoom in event #9 in 2008.

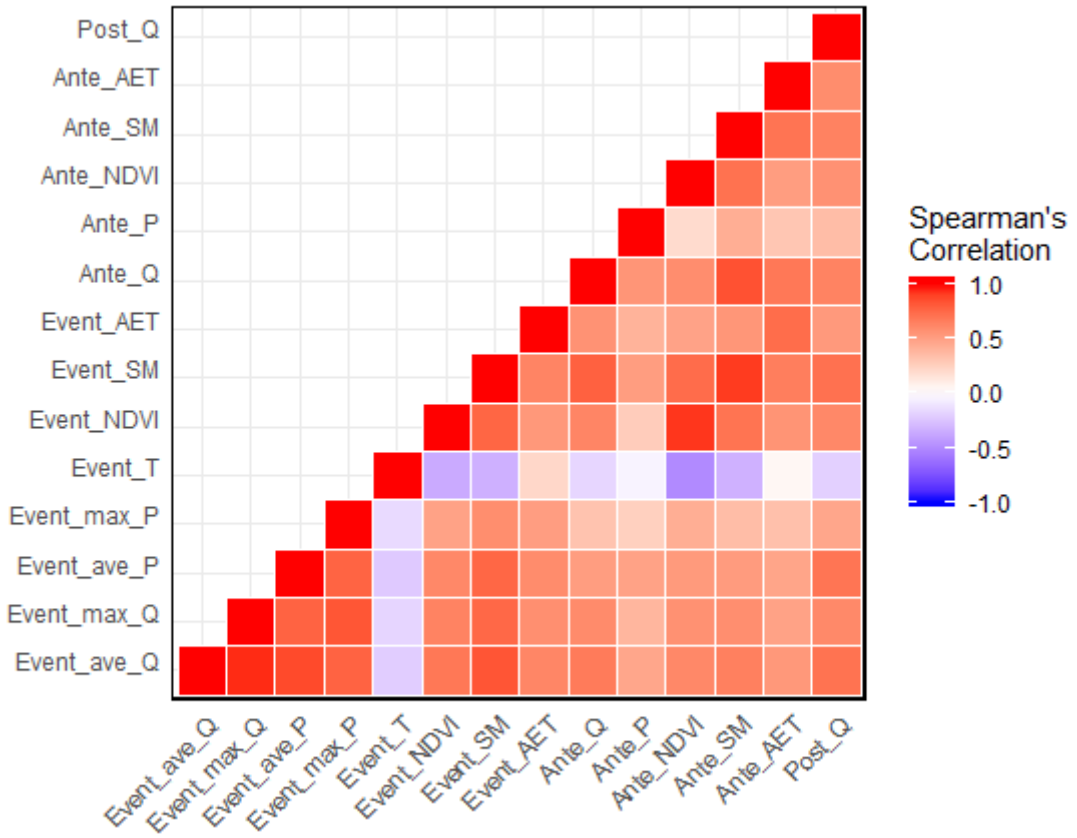

Figure B~~1~~2: Spearman's Rank correlation between 14 candidate ~~covariates~~predictors.

960

965

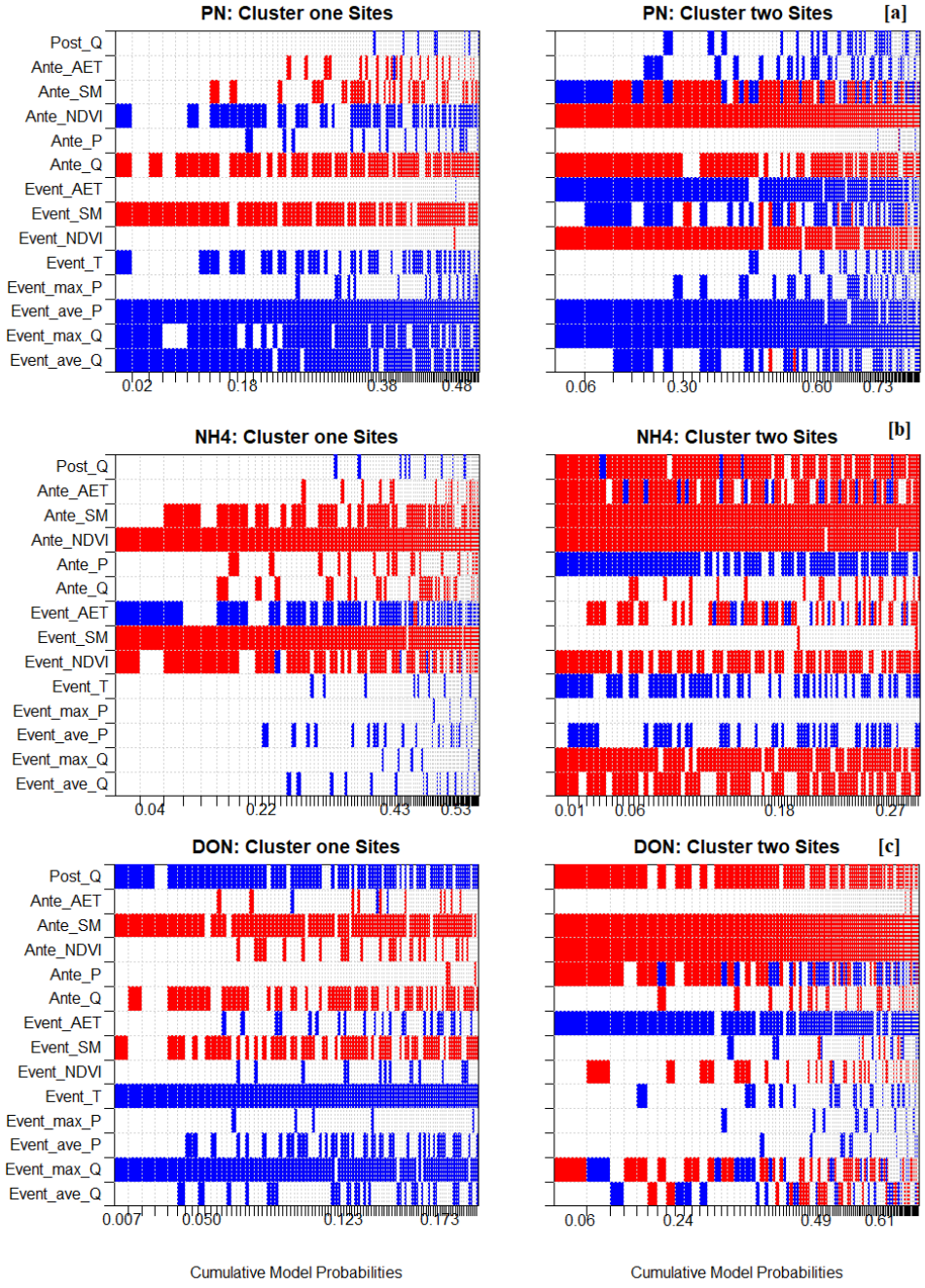

Figure ~~B2~~B3: Comparison of BMA model coefficient and cumulative model probability (top 100 models) between two clusters for: (a) PN, (b) NH_4 and (c) DON. Left - cluster one sites and Right – cluster two sites. ~~The order of predictors on the y-axis was ranked based on the posterior inclusion probability.~~ Each column in the heatmap represents the one specific model (ranked from highest model probability) and the width of the column is normalised by the posterior model probability. The colour indicates the direction of the coefficients, red – negative and blue – positive. Note: the coefficient value was averaged across the posterior median value of site-specific coefficient within each cluster (effect size, $\theta_{n,j}$, in Eq. (6)).

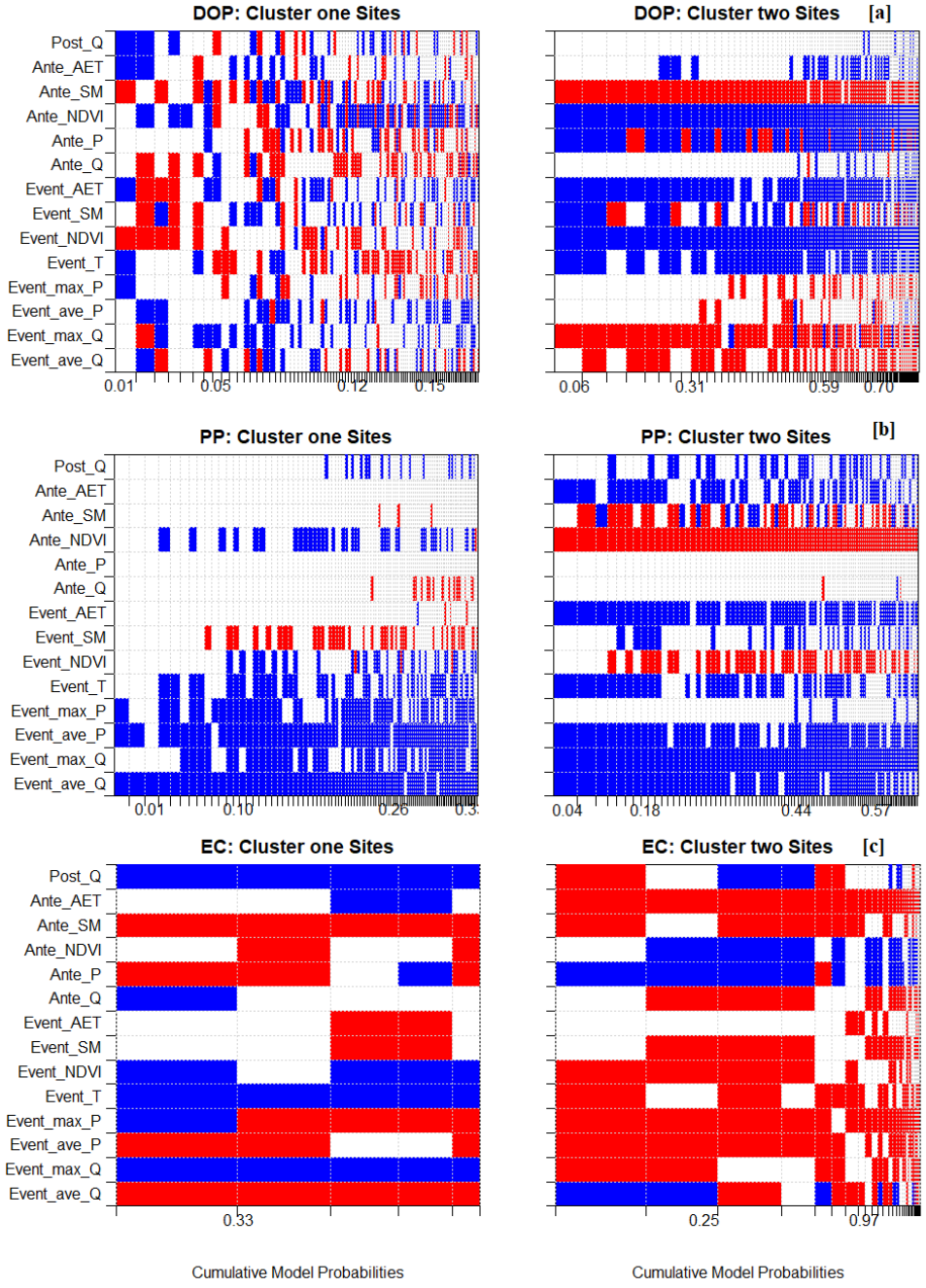

Figure B34: Comparison of BMA model coefficient and cumulative model probability (top 100 models) between two clusters for: (a) DOP, (b) PP and (c) EC. Left - cluster one sites and Right – cluster two sites. The order of predictors on the y-axis was ranked based on the posterior inclusion probability. Each column in the heatmap represents the one specific model (ranked from highest model probability) and the width of the column is normalised by the posterior model probability. The colour indicates the direction of the coefficients, red – negative and blue – positive. Note: the coefficient value was averaged across the posterior median value of site-specific coefficient within each cluster (effect size, $\theta_{n,j}$, in Eq. (6)).

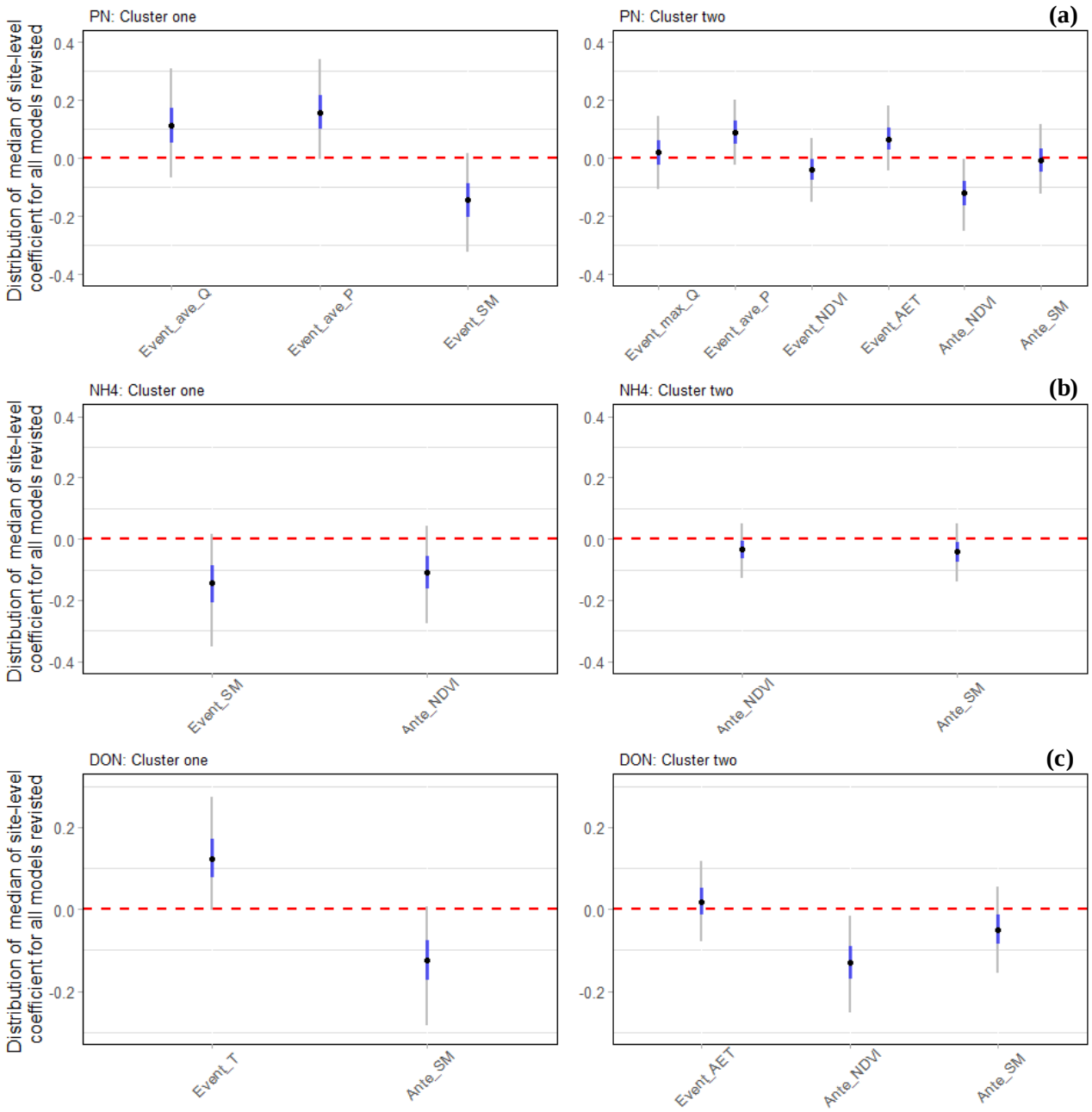

Figure ~~B4~~B5: Distribution of median of site-level coefficients for all plausible models in BMA. (a) PN, (b) NH_4 and (c) DON. Only predictors with PIP > 0.8 are included. For each specific model structure, the coefficient value of a predictor was the median of site-specific coefficient across all sites (effect size, $\theta_{n,j,}$ in Eq. (6). The distribution of this value thus represents the probability of the model (PMP), as well as variability in the same predictor across different sites. Note: black dots indicate the median; grey

vertical lines indicate 95% CI and blue coloured vertical lines indicates 50% CI. The definition of abbreviation of each predictor can be found in Table 3.

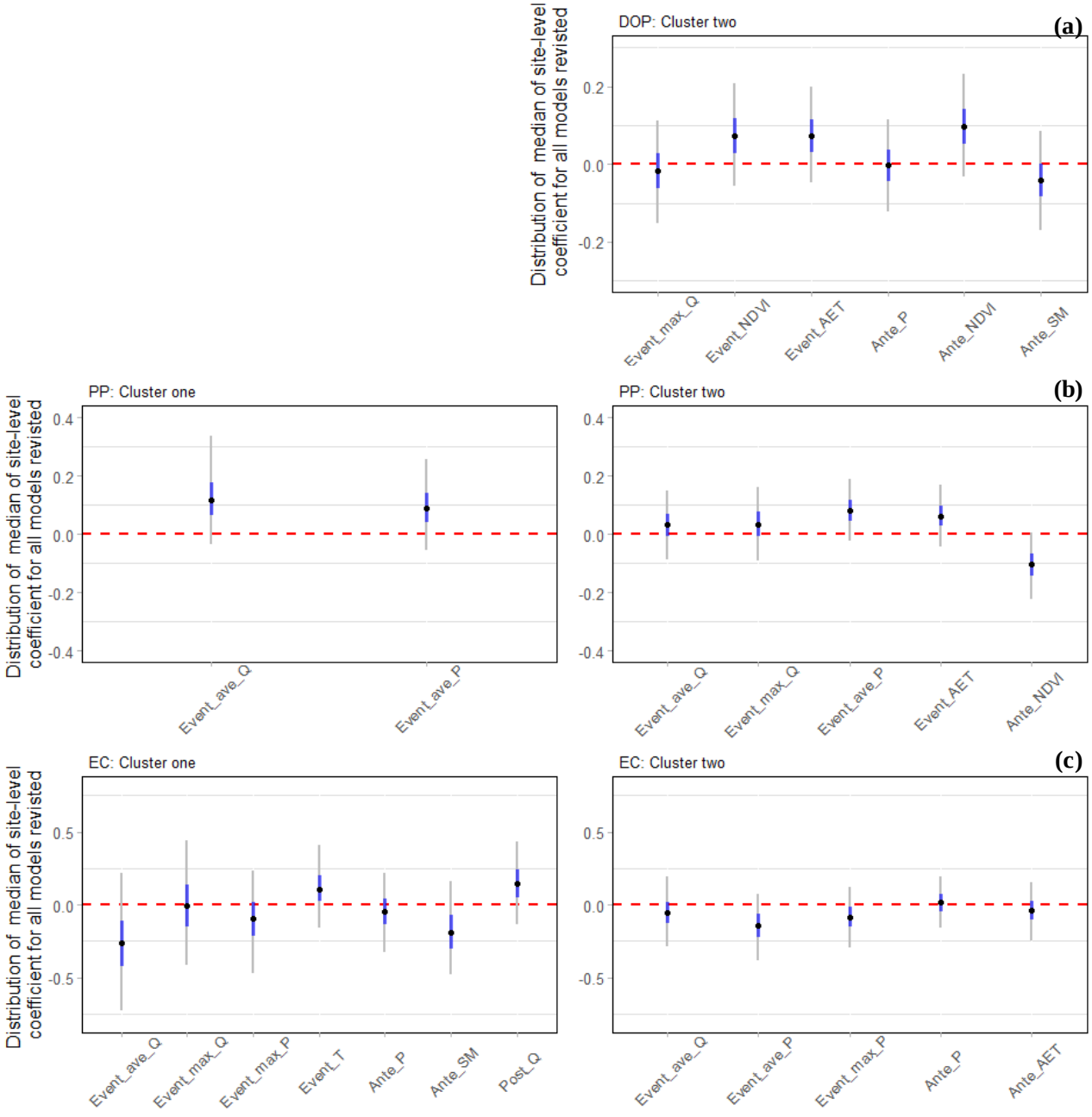

990 **Figure ~~B5~~B6: Distribution of median of site-level coefficients for all plausible models in BMA. (a) DOP, (b) PP and (c) EC. Only predictors with PIP > 0.8 are included. For each specific model structure, the coefficient value of a predictor was the median of**

site-specific coefficient across all sites (effect size, $\theta_{n,j,}$ in Equation 6). The distribution of this value thus represents the probability of the model (PMP), as well as variability in the same predictor across different sites. Note: black dots indicate the median; grey vertical lines indicate 95% CI and blue coloured vertical lines indicates 50% CI. The definition of abbreviation of each predictor can be found in Table 3.

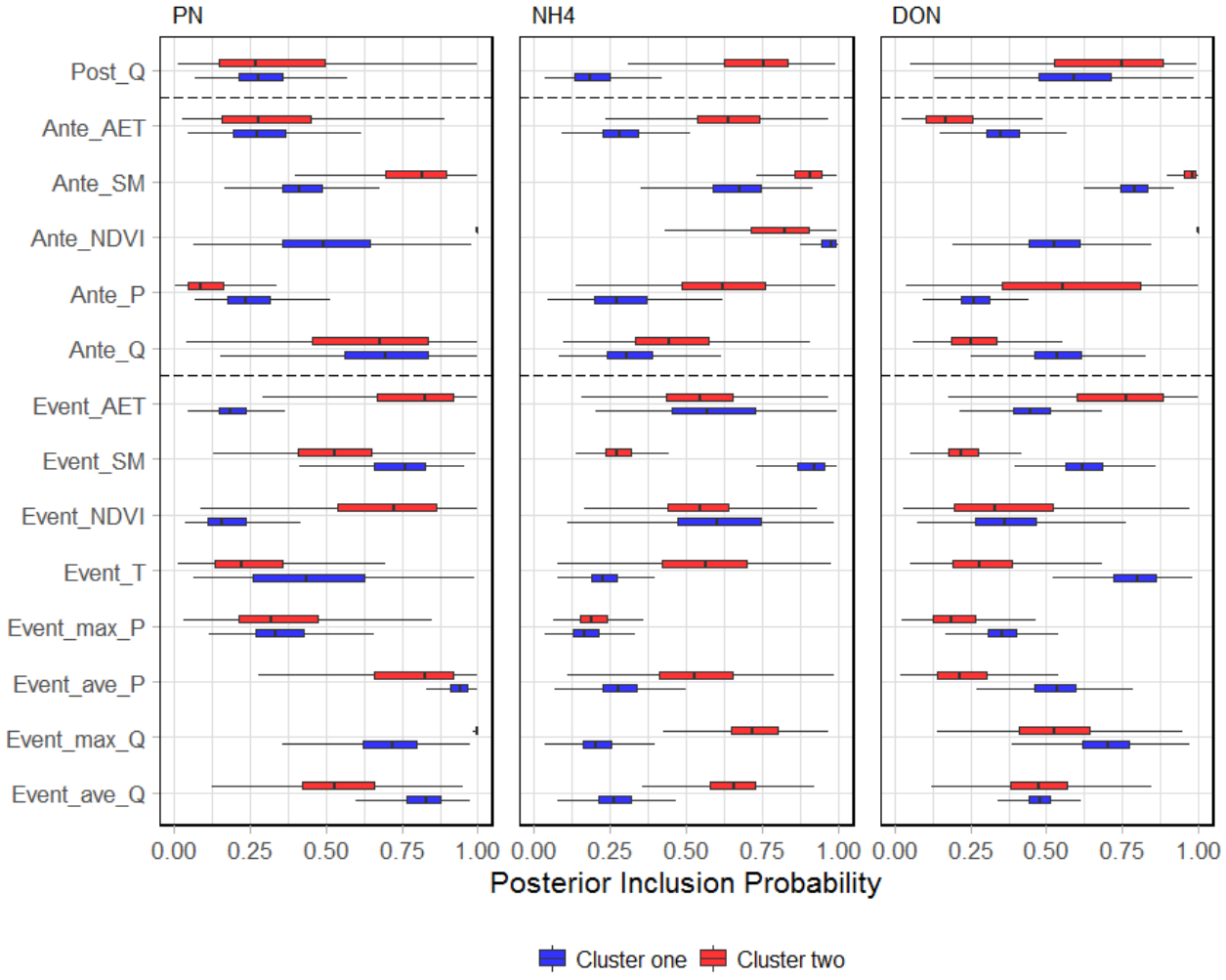

Figure ~~B6~~B7: The comparisons of distribution of posterior inclusion probability of individual predictors derived from 1,000 subsampled BMA runs. The interpretation of boxplot is the same as ~~Figure~~ Fig. 97. *Note*: colour represents different clusters: blue - Cluster and red - Cluster two. The definition of abbreviation of each predictor can be found in Table 3.

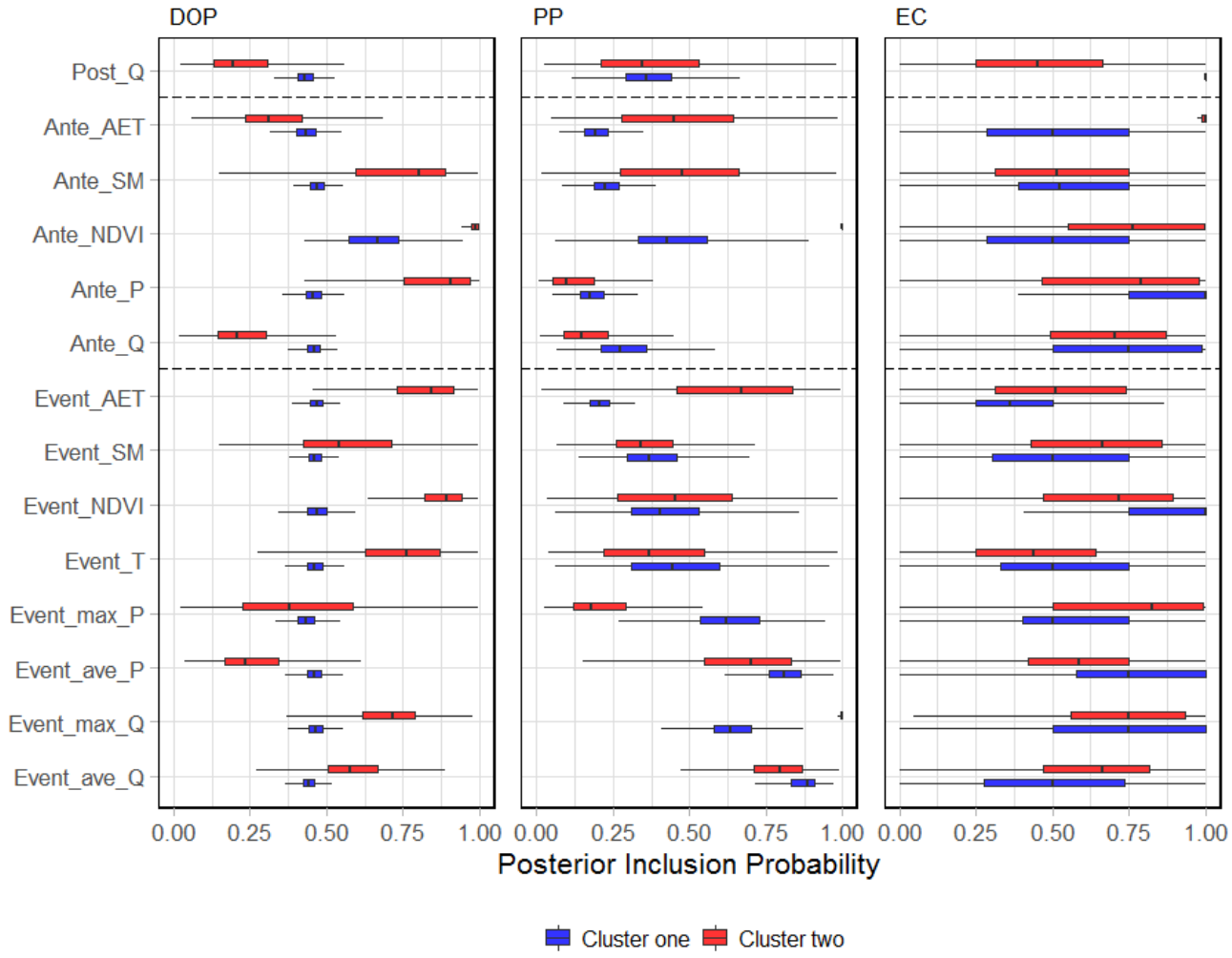

Figure ~~B7~~B8: The comparisons of distribution of posterior inclusion probability of individual predictors derived from 1,000 subsampling BMA. The interpretation of boxplot is the same as ~~Figure~~ Fig. ~~3~~7. *Note*: colour represents different clusters: blue - Cluster and red - Cluster two.

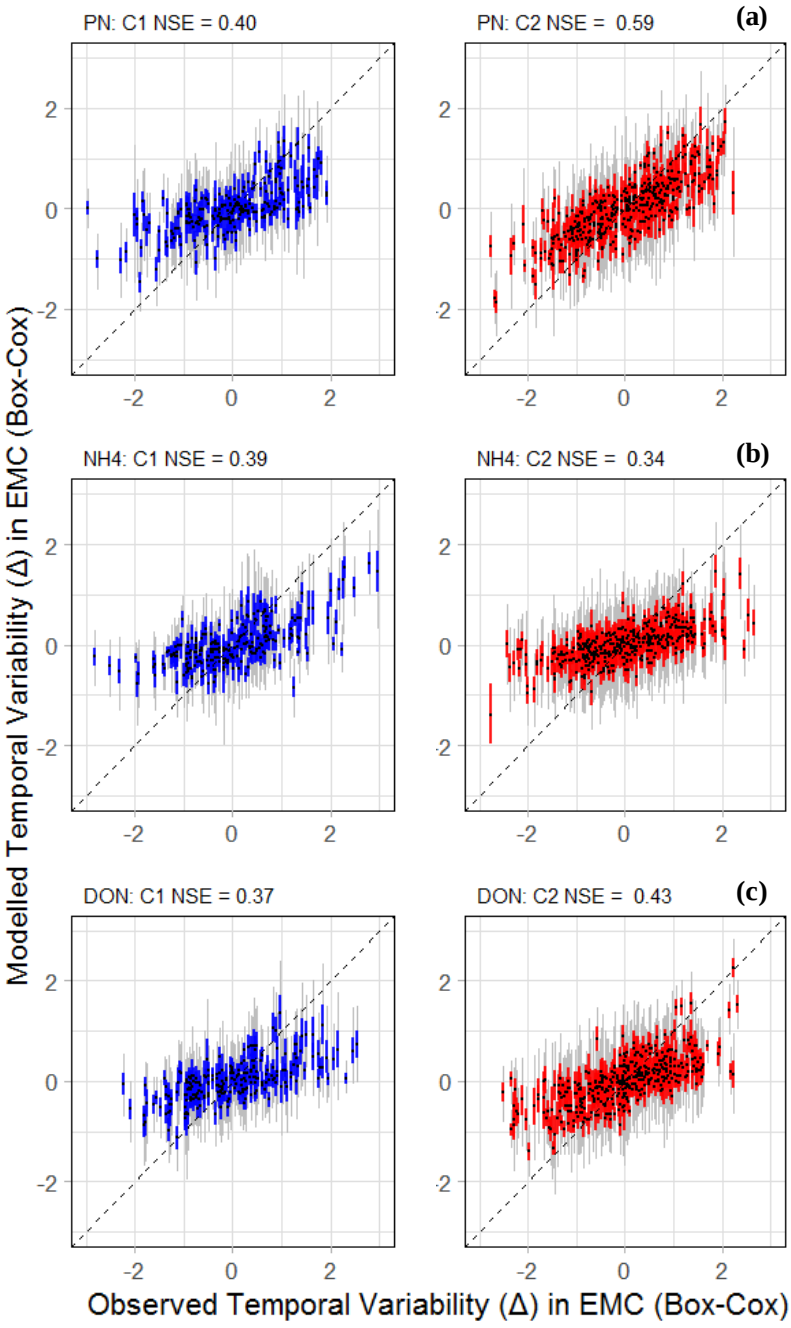

Figure B98: Performance of the BMA models of the temporal variability of nine constituents across 32 sites, represented by prediction intervals from BMA and observed Box-Cox EMC across two clusters of sites for: (a) PN; (b) NH_4 and (c) DON. The NSE values are calculated based on predictions within group- (cluster) level. *Note*: black dots are the prediction median; grey vertical lines are the 95% CI and coloured vertical lines indicates 50% CI: blue - Cluster and red - Cluster two. The dashed black lines is the 1:1 relationship.

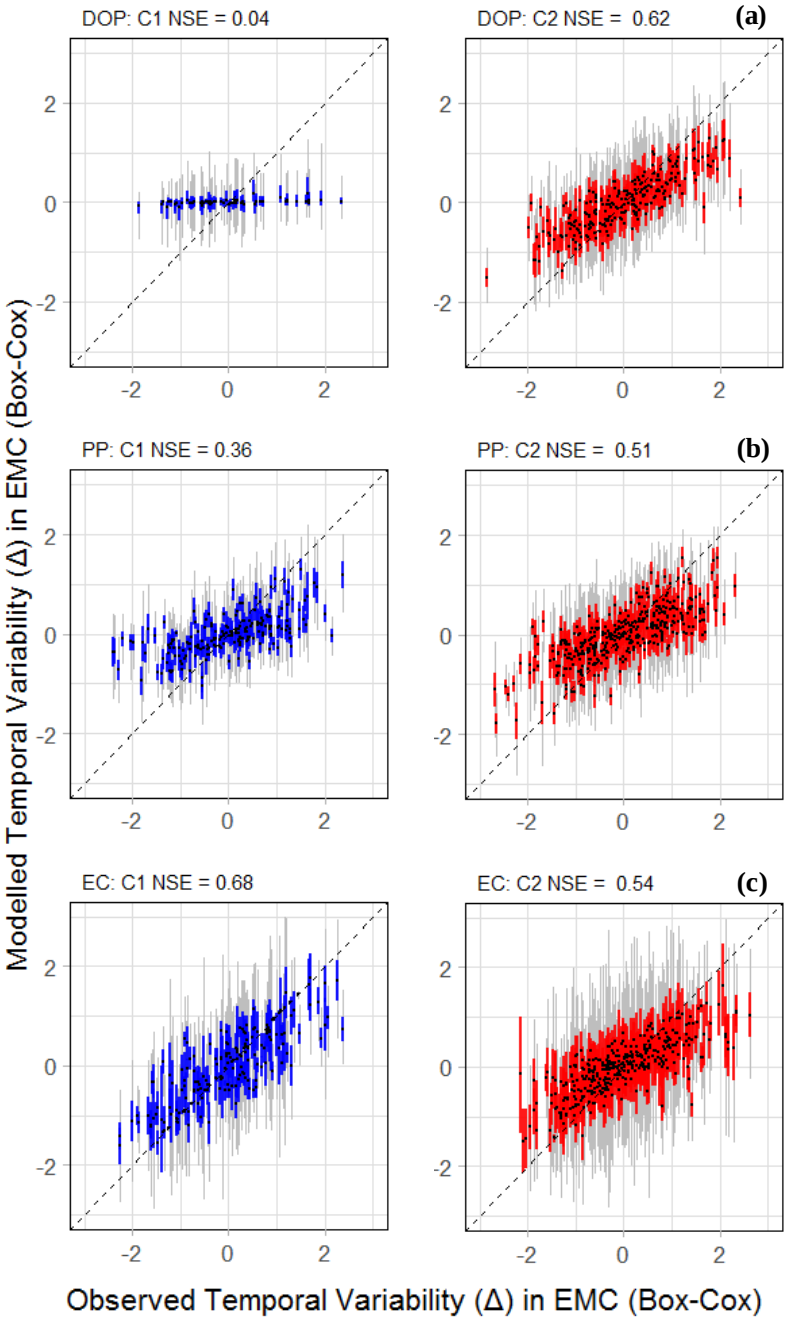

Figure B10: Performance of the BMA models of the temporal variability of nine constituents across 32 sites, represented by prediction intervals from BMA and observed Box-Cox EMC across two clusters of sites for: (a) DOP; (b) PP and (c) EC. The NSE values are calculated based on predictions within group- (cluster) level. *Note*: black dots are the prediction median; grey vertical lines are the 95% CI and coloured vertical lines indicates 50% CI: blue - Cluster and red - Cluster two. The dashed black lines is the 1:1 relationship.

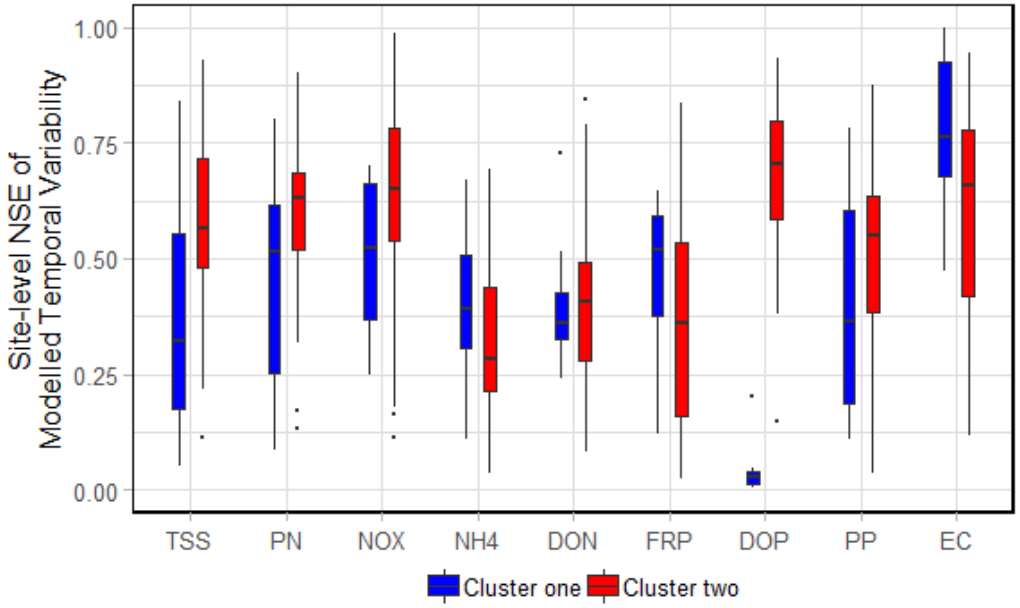

Figure B11: Distribution of site-level NSE for modelled the temporal variability of two clusters of sites. The interpretation of boxplot is the same as Fig. 7. NSE values were calculated based on site-level predictions of event median EMC; blue is Cluster 1("wet"); and red is Cluster 2 ("dry") (i.e., each boxplot is comprised of respective number of sites in each cluster, one for each catchment).

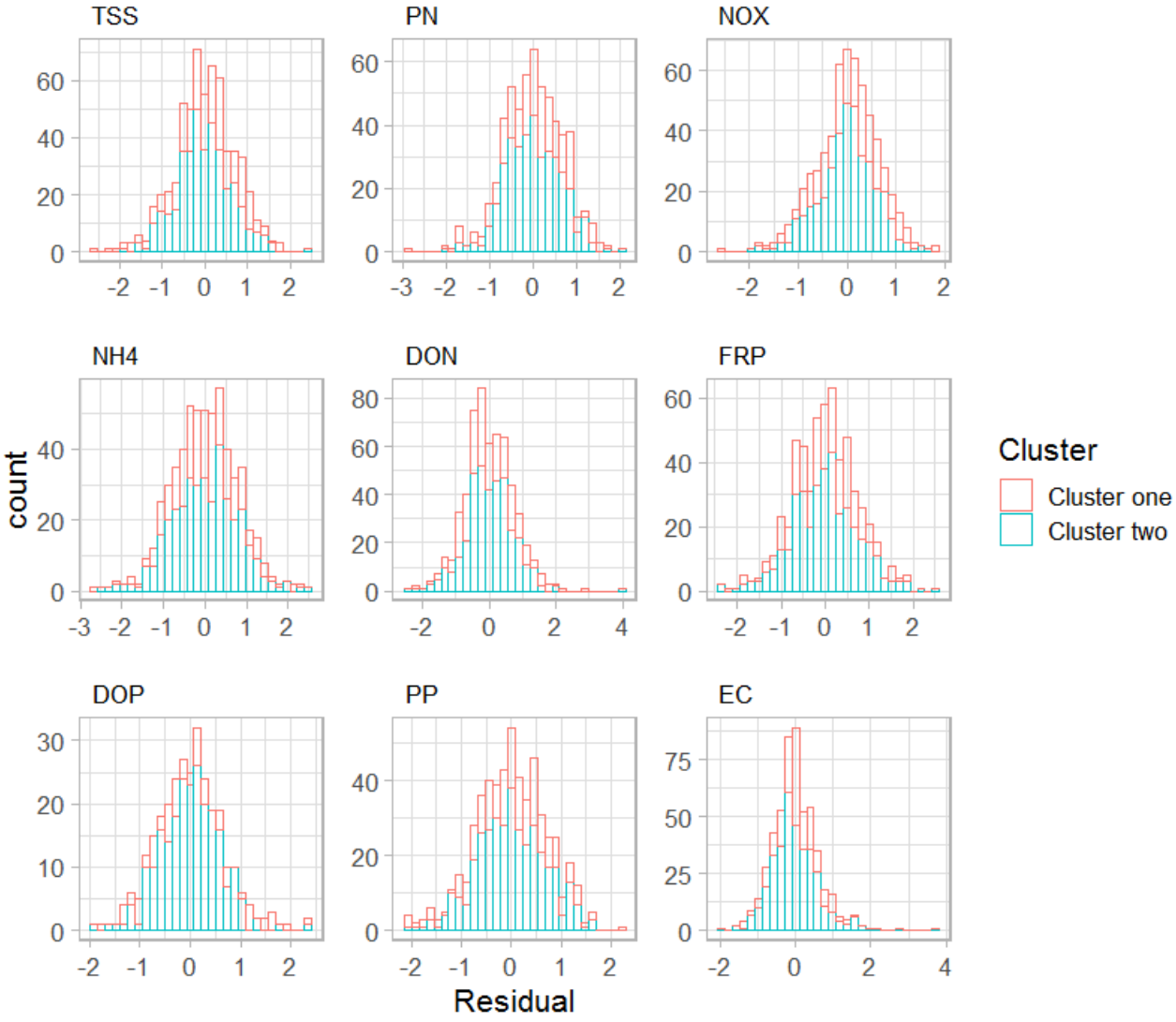

Figure ~~B10~~B12: Histograms showing distribution of residuals of nine constituents from BMA predictions. Red – Cluster one; Blue – Cluster two.

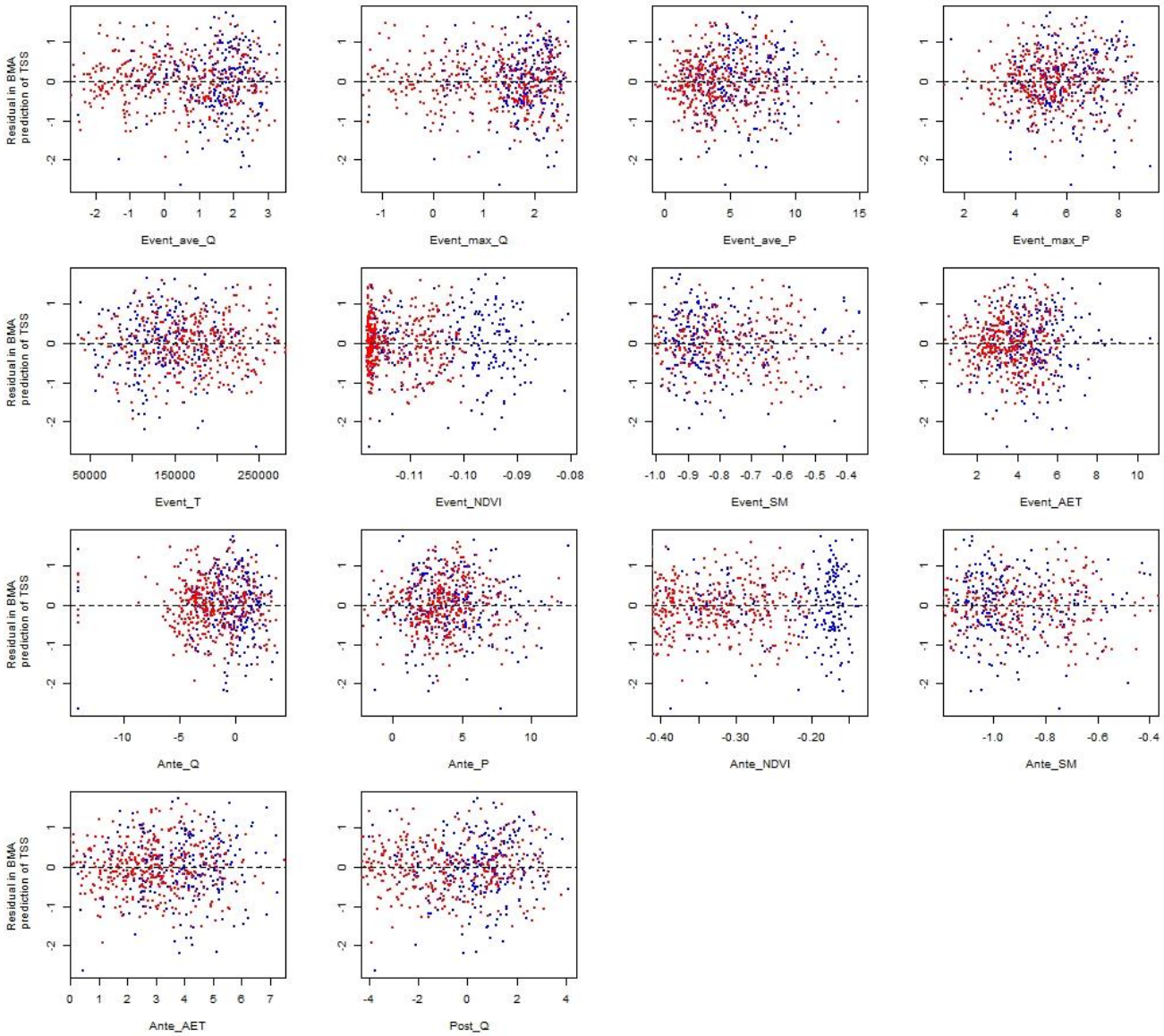

Figure ~~B11~~B13: Relationship between residual in median of BMA prediction of TSS and 14 candidate covariates in BMA. Note, difference colours indicate two clusters: Red – Cluster one; Blue – Cluster two.

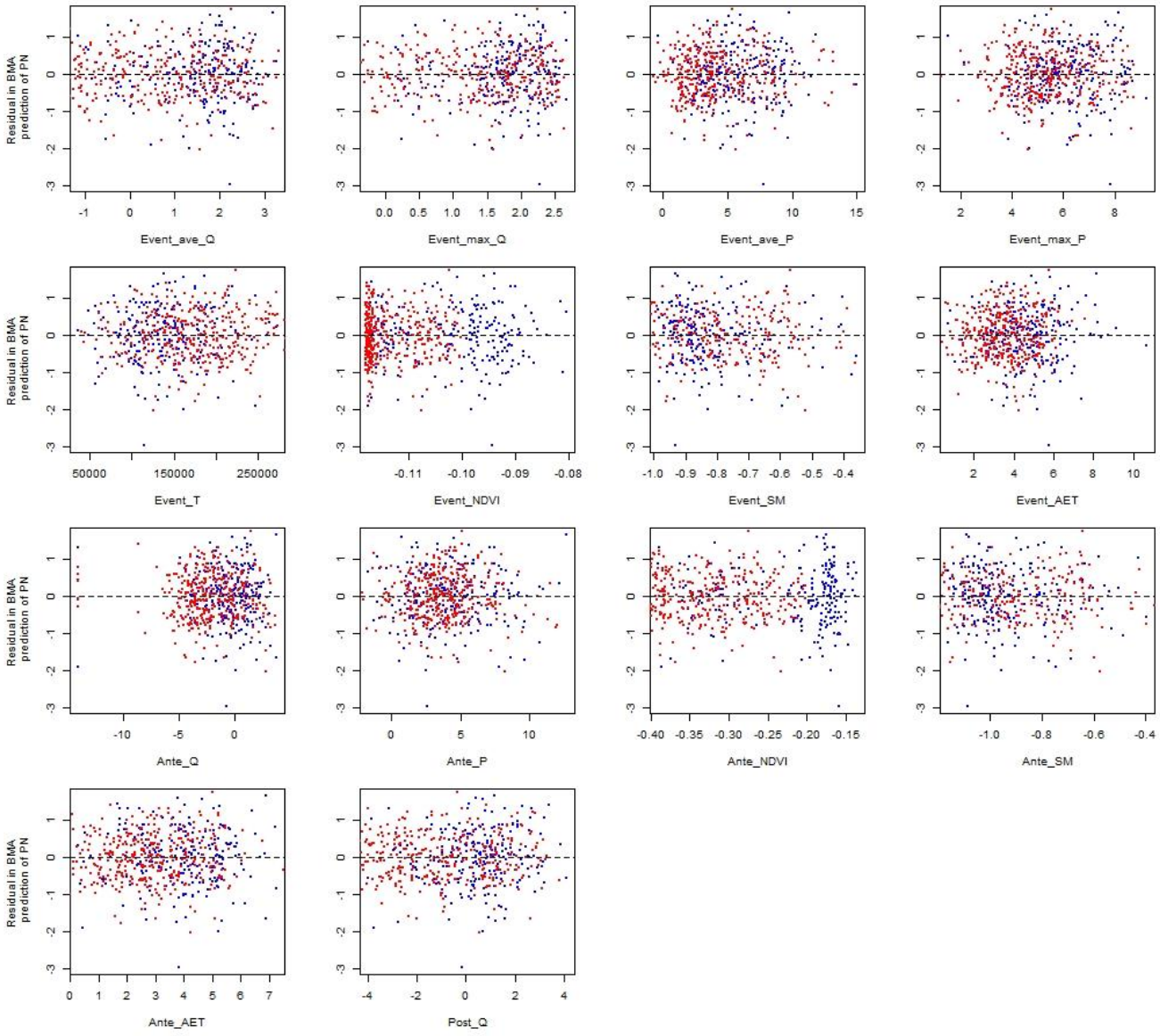

Figure ~~B12~~B14: Relationship between residual in median of BMA prediction of PN and 14 candidate covariates in BMA. Note, difference colours indicate two clusters: Red – Cluster one; Blue – Cluster two.

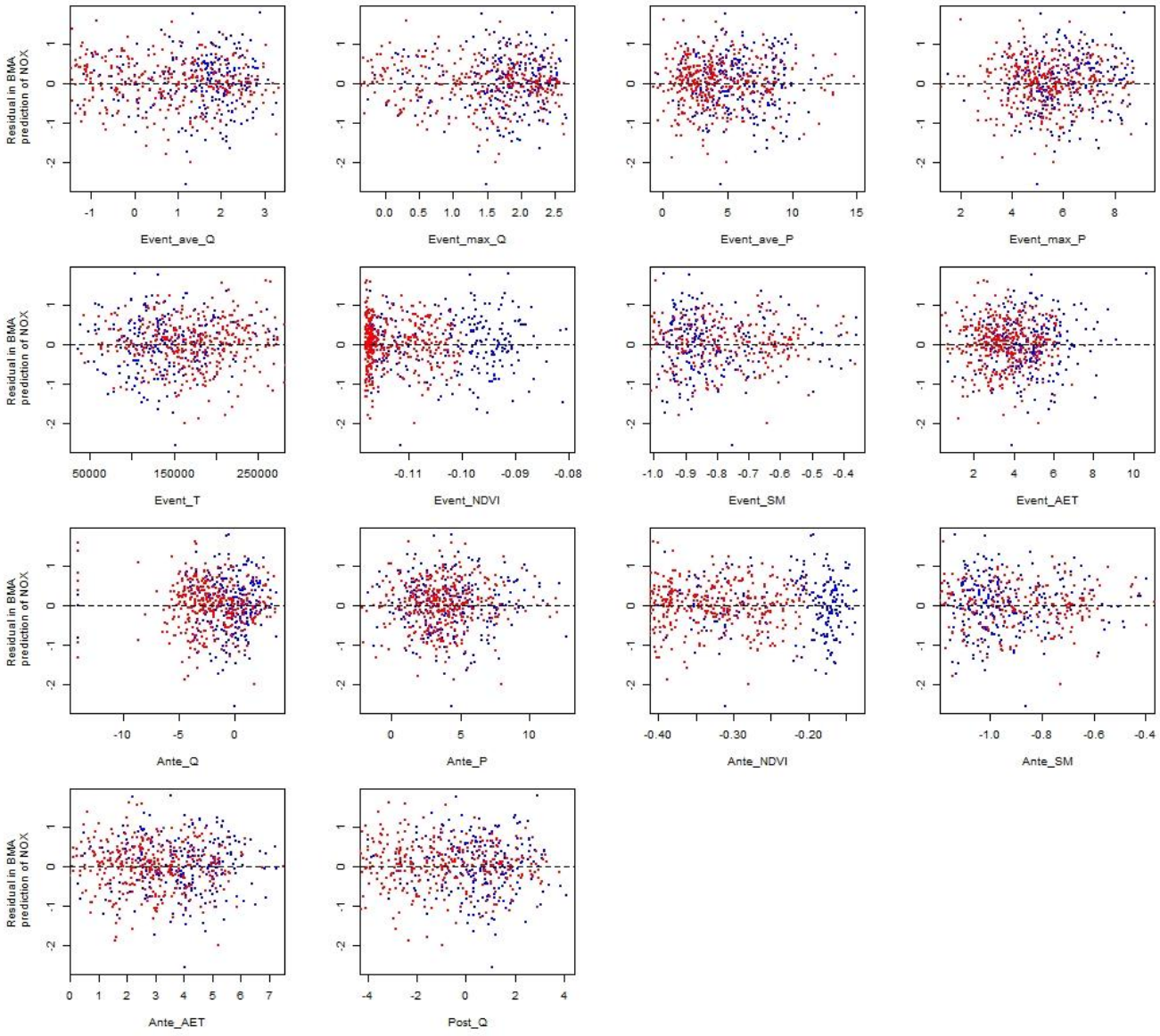

Figure ~~B13~~B15: Relationship between residual in median of BMA prediction of NO_X and 14 candidate covariates in BMA. Note, difference colours indicate two clusters: Red – Cluster one; Blue – Cluster two.

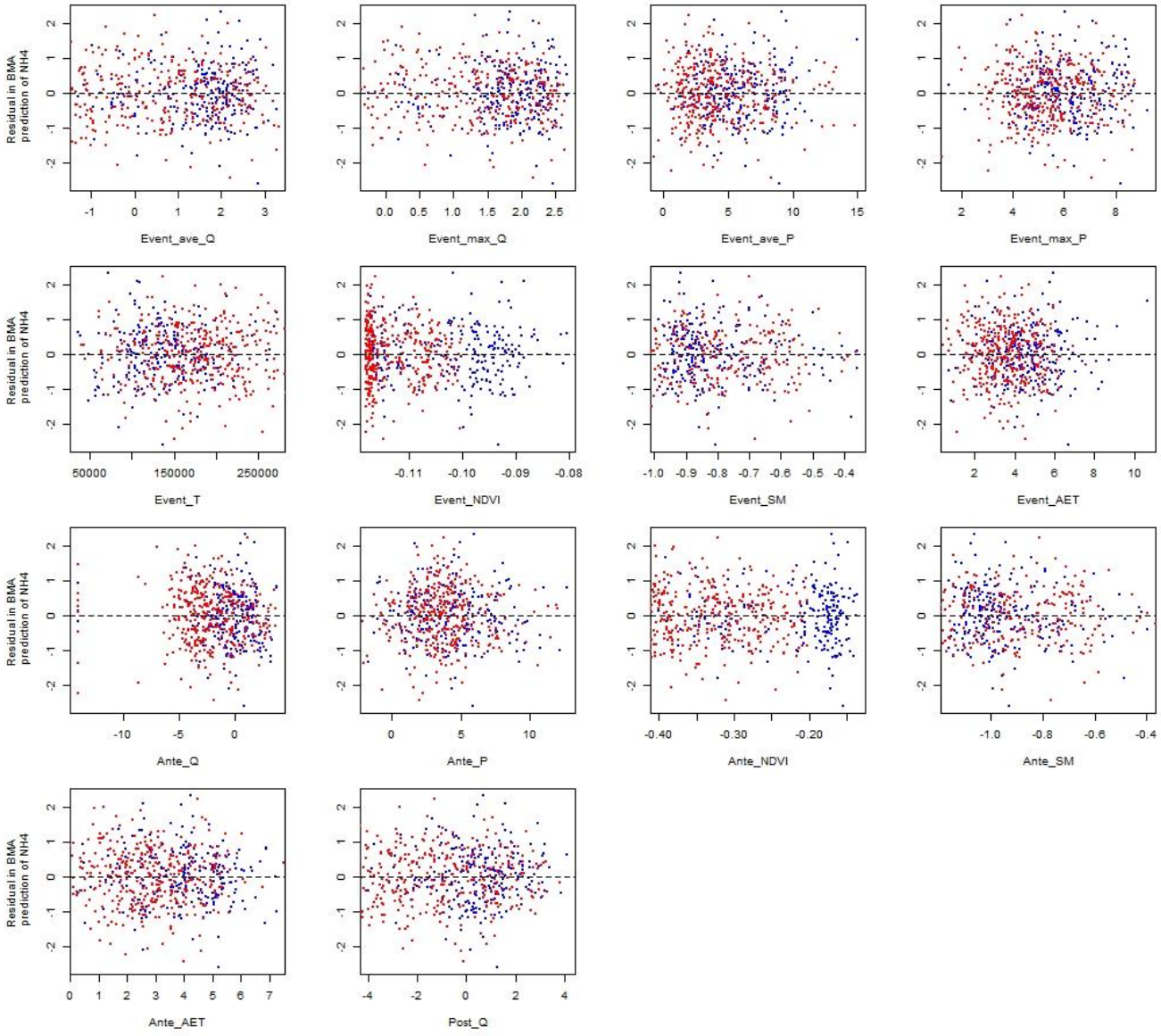

Figure ~~B14~~B16: Relationship between residual in median of BMA prediction of NH_4 and 14 candidate covariates in BMA. Note, difference colours indicate two clusters: Red – Cluster one; Blue – Cluster two.

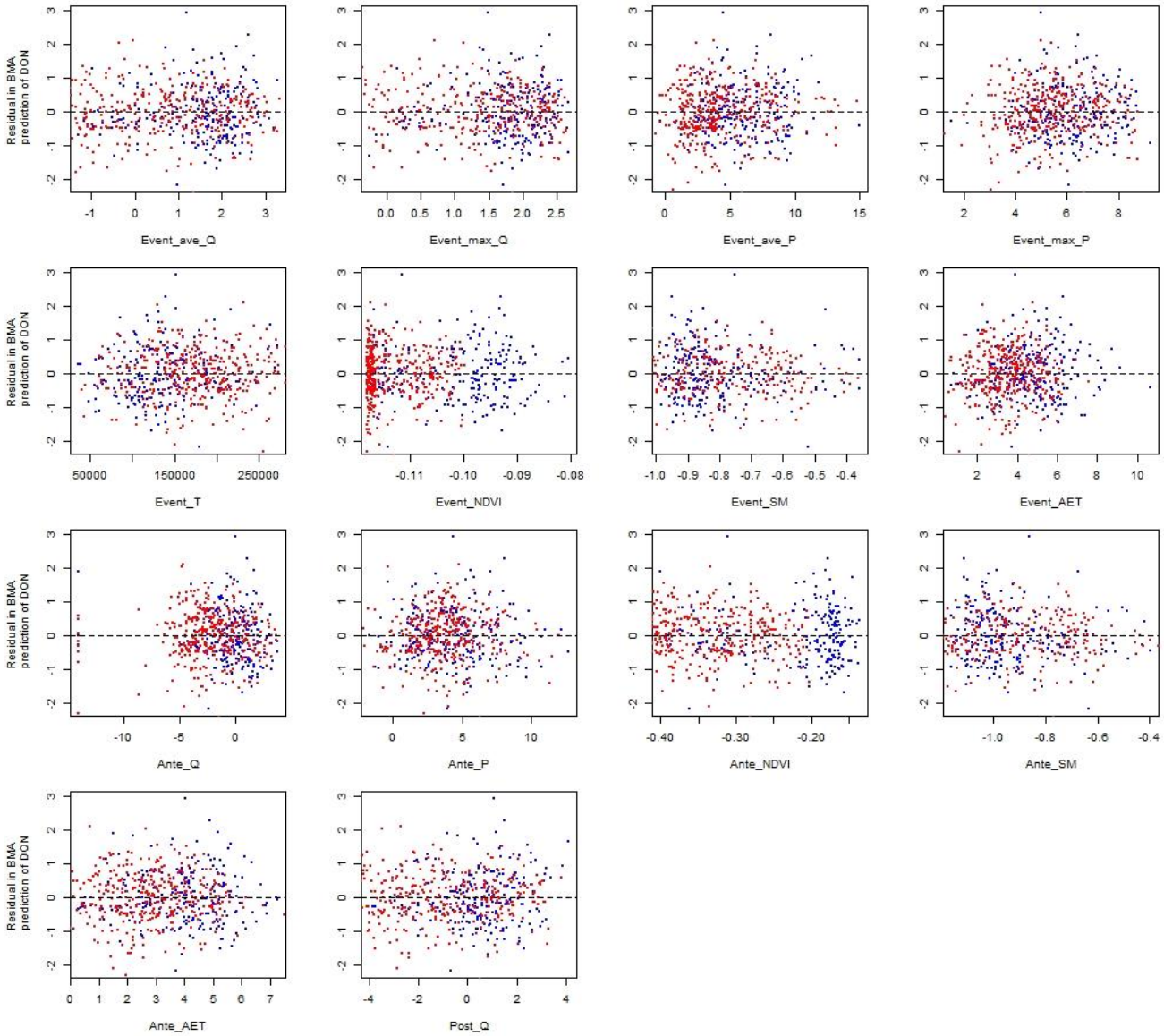

Figure ~~B15~~B17: Relationship between residual in median of BMA prediction of DON and 14 candidate covariates in BMA. Note, difference colours indicate two clusters: Red – Cluster one; Blue – Cluster two.

1060

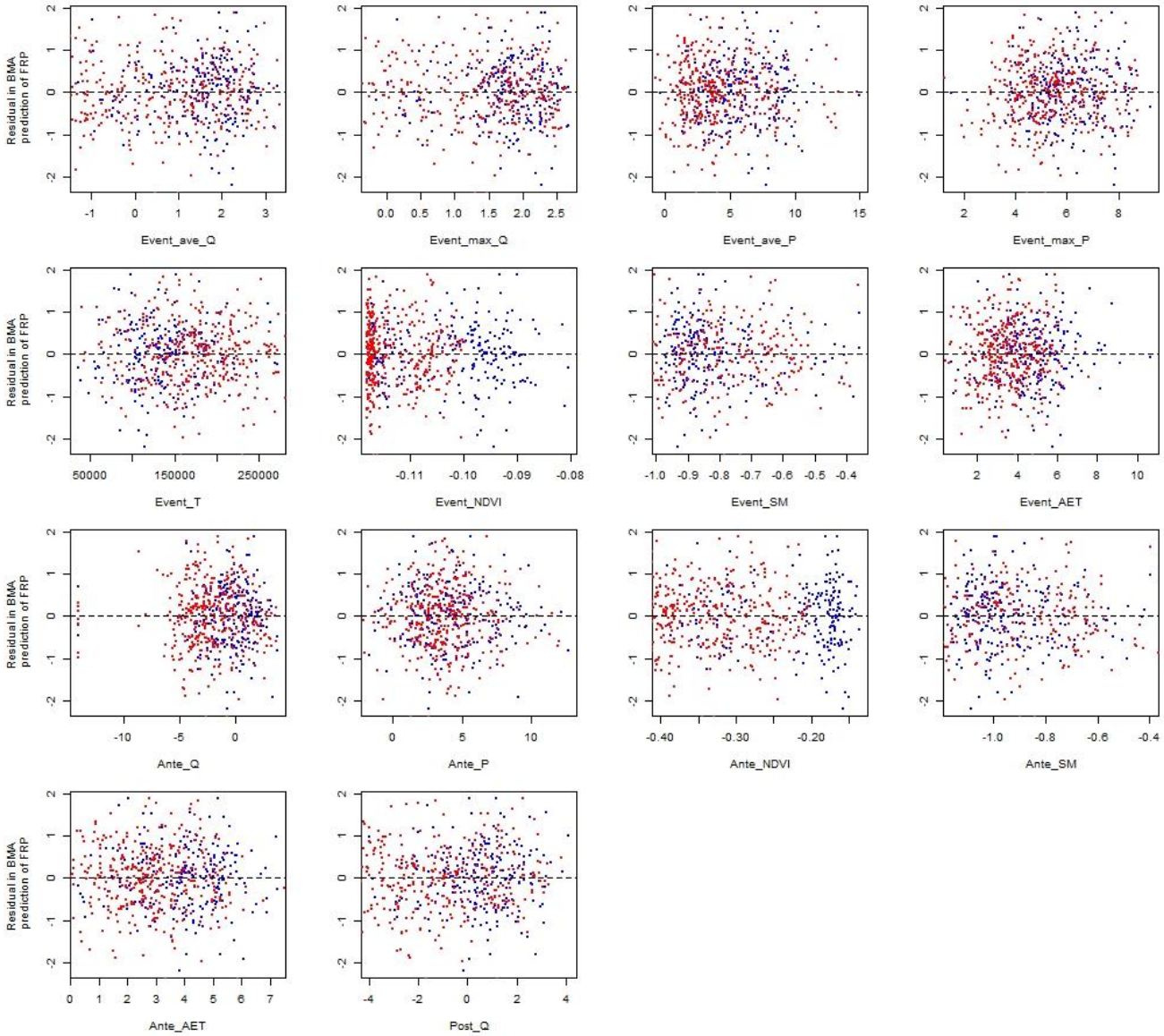

Figure ~~B16~~B18: Relationship between residual in median of BMA prediction of FRP and 14 candidate covariates in BMA. Note, difference colours indicate two clusters: Red – Cluster one; Blue – Cluster two.

1065

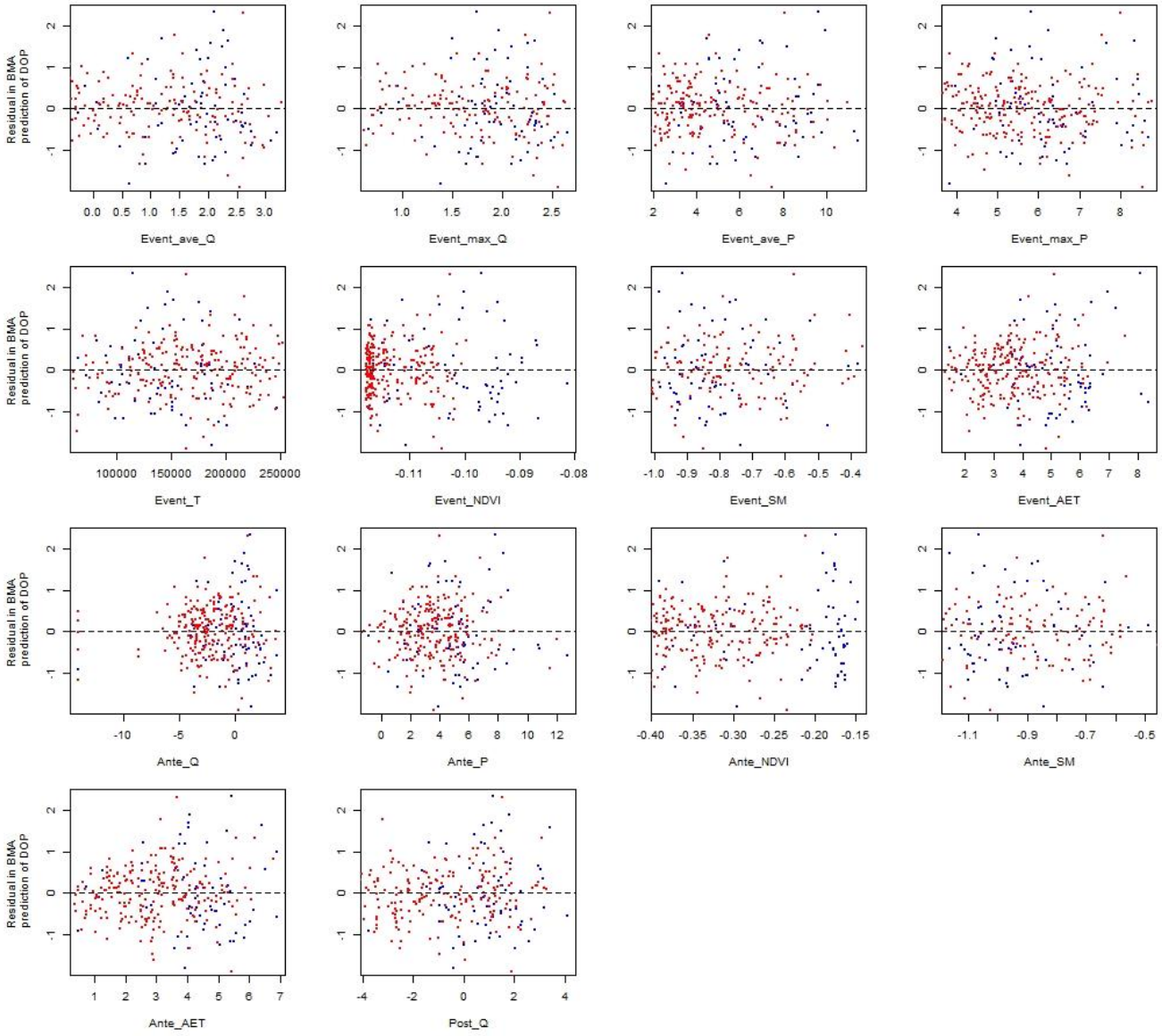

Figure ~~B17~~B19: Relationship between residual in median of BMA prediction of DOP and 14 candidate covariates in BMA. Note, difference colours indicate two clusters: Red – Cluster one; Blue – Cluster two.

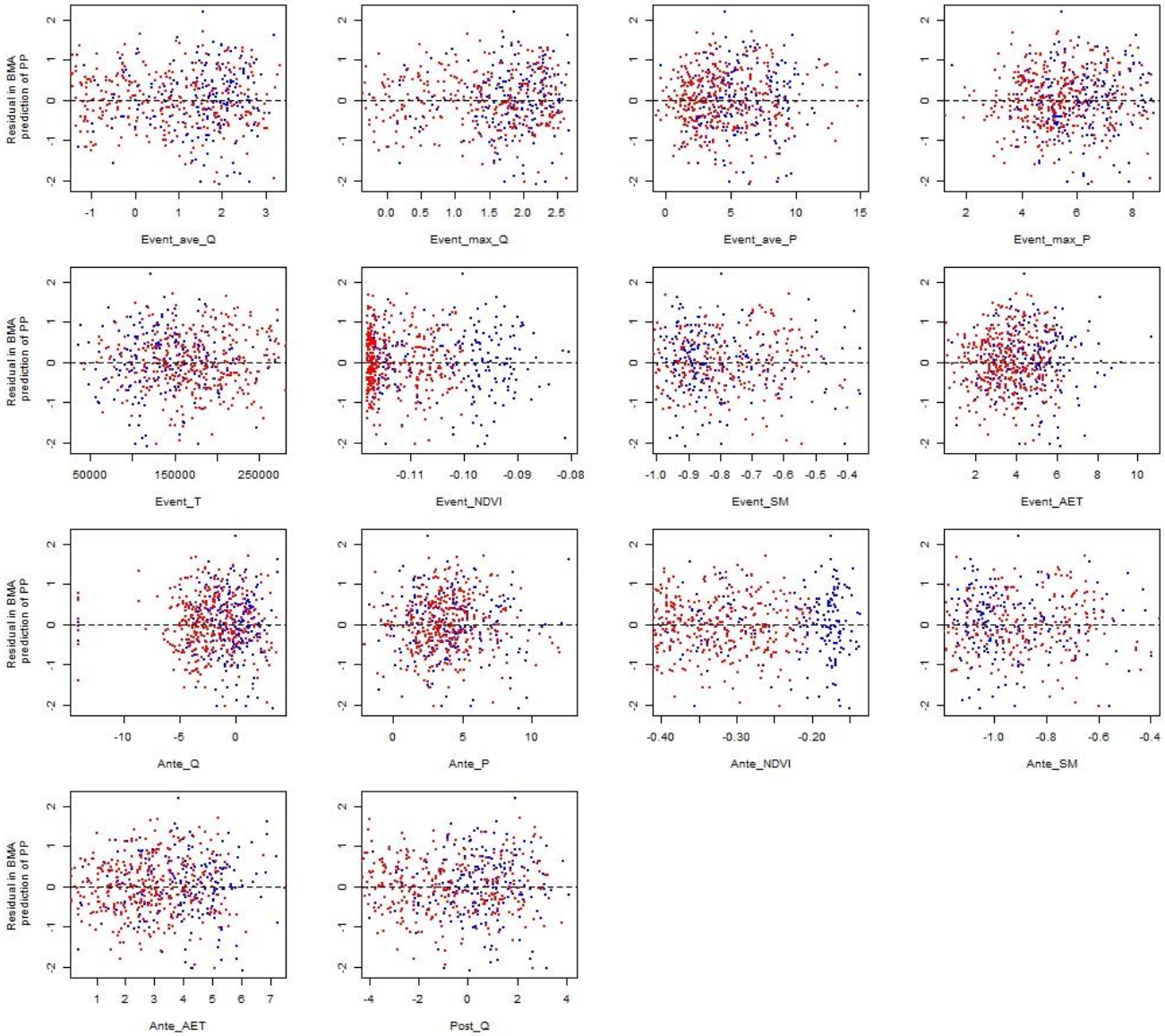

Figure ~~B18~~B20: Relationship between residual in median of BMA prediction of PP and 14 candidate covariates in BMA. Note, difference colours indicate two clusters: Red – Cluster one; Blue – Cluster two.

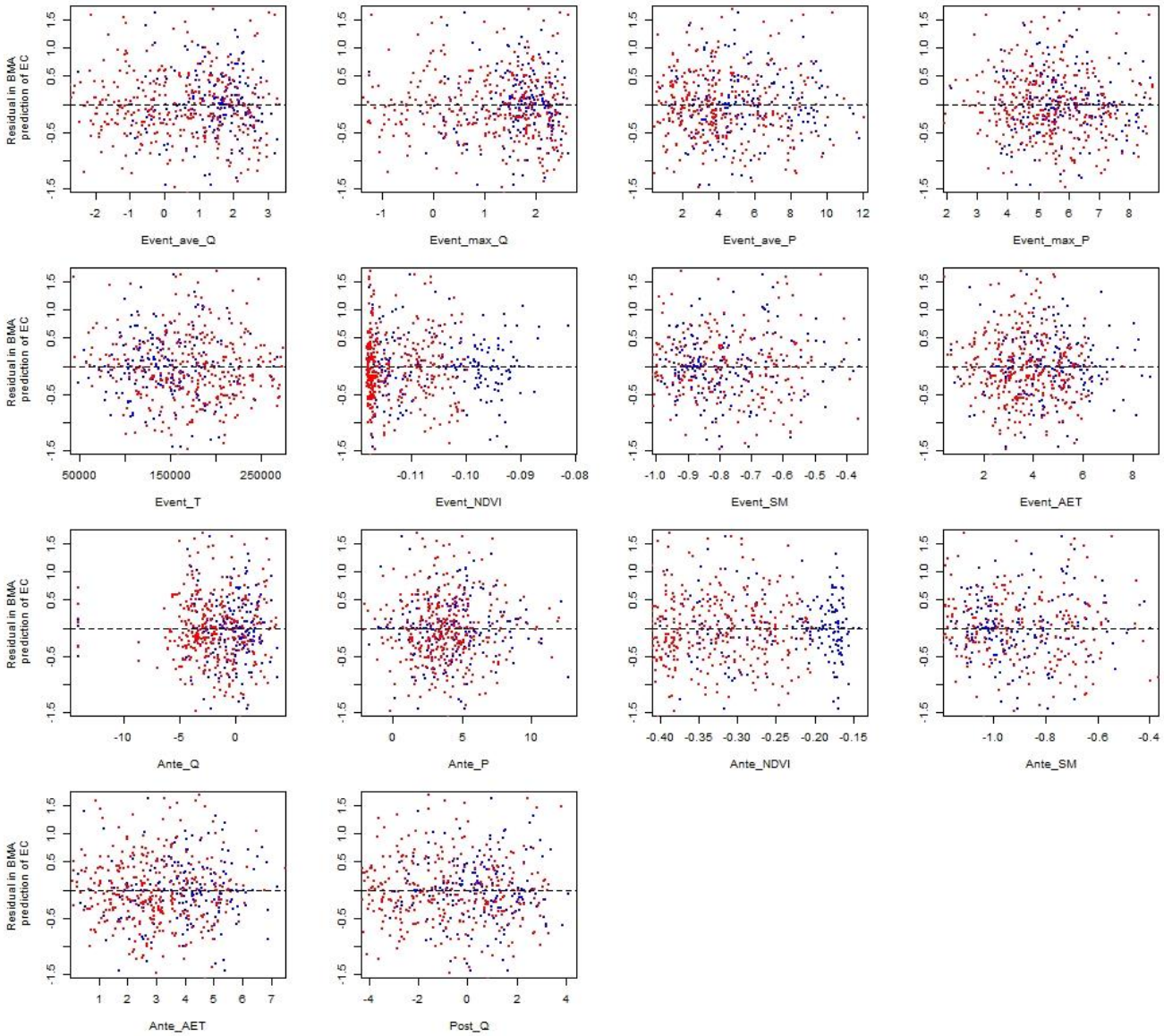

Figure ~~B19~~B21: Relationship between residual in median of BMA prediction of EC and 14 candidate covariates in BMA. Note, difference colours indicate two clusters: Red – Cluster one; Blue – Cluster two.

Appendix C - Table

Table C1. Description of 32 sites in the GBR catchments

NRM	Site ID	River and site name	Latitude/°	Longitude/°	Catchment area / km^2
Cape York	105107A	Normanby River at Kalpowar Crossing	-14.9185	144.2100	12934
Wet tropics	110001D	Barron River at Myola	-16.7998	145.6121	1945
Wet tropics	110002A	Barron River at Mareeba	-17.0022	145.4293	836
Wet tropics	110003A	Barron River at Picnic Crossing	-17.2591	145.5386	228
Wet tropics	1110056	Mulgrave River at Deeral	-17.2075	145.9264	785
Wet tropics	1111019	Russell River at East Russell	-17.2672	145.9544	524
Wet tropics	1120049	North Johnstone River at Old Bruce Hwy Bridge (Goondi)	-17.5059	145.9920	959
Wet tropics	112004A	North Johnstone River at Tung Oil	-17.5456	145.9325	925
Wet tropics	112101B	South Johnstone River at Upstream Central Mill	-17.6106	145.9789	400
Wet tropics	113006A	Tully River at Euramo	-17.9936	145.9411	1450
Wet tropics	113015A	Tully River at Tully Gorge National Park	-17.7727	145.6507	482
Wet tropics	116001F	Herbert River at Ingham	-18.6328	146.1427	8581
Burdekin	119101A	Barratta Creek at Northcote	-19.6923	147.1688	753
Burdekin	120001A	Burdekin River at Home Hill	-19.6436	147.3958	129939
Burdekin	120002C	Burdekin River at Sellheim	-20.0078	146.4369	36290
Burdekin	120301B	Belyando River at Gregory Development Rd.	-21.5423	146.8656	35410
Burdekin	120302B	Cape River at Taemas	-20.9996	146.4271	16070
Burdekin	120310A	Suttor River at Bowen Developmental Road	-21.5375	147.0424	10760
Mackay Whitsunday	124001B	O'Connell River at Stafford's Crossing	-20.6526	148.5730	342
Mackay Whitsunday	1240062	O'Connell River at Caravan Park	-20.5664	148.6117	825
Mackay Whitsunday	125013A	Pioneer River at Dumbleton Pump Station	-21.1441	149.0753	1485
Mackay Whitsunday	126001A	Sandy Creek at Homebush	-21.2831	149.0228	326
Fitzroy	1300000	Fitzroy River at Rockhampton	-23.3175	150.4819	139159
Fitzroy	130206A	Theresa Creek at Gregory Highway	-23.4292	148.1514	8485
Fitzroy	130302A	Dawson River at Taroom	-25.6376	149.7901	15850
Fitzroy	130504B	Comet River at Comet Weir	-23.6125	148.5514	16460
Burnett Mary	136002D	Burnett River at Mt Lawless	-25.5447	151.6549	29360
Burnett Mary	136004A	Jones Weir HW	-25.5948	151.2964	21700
Burnett Mary	136014A	Burnett River at Ben Anderson Barrage Head Water	-24.8896	152.2922	32891
Burnett Mary	136094A	Burnett River at Jones Weir (TW)	-25.5948	151.2974	21700

Burnett Mary	136106A	Burnett River at Eidsvold	-25.4023	151.1033	7117
Burnett Mary	138014A	Mary River at Home Park	-25.7683	152.5274	6845

Table C2. Parameters for running the Hydrun toolbox

Filter coefficient	Pass for baseflow separation	Peak discharge threshold	Return ratio	Smooth coefficient	Minimum duration
0.975	3	100	0.01	6	24

Table C3. Average number of samples per event for each constituent

TSS	PN	NO_X	NH_4	DON	FRP	DOP	PP	EC
15	14	14	14	14	15	12	14	16

Table C~~4~~2. Number of EMCs for each constituent

Cluster	TSS	PN	NO_X	NH_4	DON	FRP	DOP	PP	EC
One	225	207	218	217	215	210	66	186	174
Two	381	370	372	370	373	372	231	366	354
% of event monitored	43	41	42	42	42	41	21	39	37

Table C~~3~~C5. Posterior inclusion probability of individual predictor derived from BMA on two clusters of sites.

Predictor	TSS		PN		NO_X		NH_4		DON		FRP		DOP		PP		EC	
	Cluster one	Cluster two	Cluster one	Cluster two	Cluster one	Cluster two	Cluster one	Cluster two	Cluster one	Cluster two	Cluster one	Cluster two	Cluster one	Cluster two	Cluster one	Cluster two	Cluster one	Cluster two
Event_ave_Q	*0.93*	0.47	*0.87*	0.49	*0.97*	0.56	0.21	0.68	0.47	0.47	0.33	0.38	0.46	0.58	*0.92*	*0.85*	*1.00*	*0.86*
Event_max_Q	0.73	*1.00*	0.76	*1.00*	0.33	0.58	0.14	0.79	0.79	0.60	*0.94*	0.43	0.46	*0.85*	0.66	*0.99*	*1.00*	0.63
Event_ave_P	*0.92*	*0.92*	*0.98*	*0.92*	0.32	0.07	0.25	0.51	0.52	0.16	0.79	*0.96*	0.45	0.24	*0.86*	*0.82*	0.67	*0.90*
Event_max_P	0.24	0.48	0.24	0.29	0.47	0.01	0.10	0.13	0.31	0.17	0.68	0.44	0.41	0.27	0.67	0.15	*1.00*	*0.96*
Event_T	0.07	0.27	0.50	0.21	0.19	*0.98*	0.16	0.58	*0.88*	0.26	*0.86*	*0.90*	0.48	0.78	0.53	0.61	*1.00*	0.64
Event_NDVI	0.03	0.27	0.09	*0.89*	0.77	0.55	0.68	0.62	0.35	0.34	0.38	0.49	0.46	0.97	0.39	0.52	0.75	0.79
Event_SM	0.54	0.21	*0.83*	0.58	*0.99*	0.38	*0.96*	0.21	0.64	0.19	0.59	0.48	0.47	0.66	0.40	0.35	0.33	0.60
Event_AET	0.13	0.07	0.12	*0.90*	0.61	*1.00*	0.68	0.57	0.43	*0.86*	0.57	0.38	0.51	0.87	0.17	*0.81*	0.33	0.10

Ante_Q	0.23	0.18	0.76	0.76	0.15	*0.98*	0.30	0.37	0.56	0.25	0.36	*0.86*	0.47	0.17	0.25	0.12	0.33	0.59
Ante_P	0.20	0.05	0.22	0.06	0.16	0.03	0.25	0.70	0.22	0.75	0.25	*0.88*	0.44	0.98	0.13	0.06	*0.81*	*0.91*
Ante_NDVI	0.23	*1.00*	0.56	*1.00*	*0.86*	*1.00*	*0.99*	*0.89*	0.47	*1.00*	*0.97*	*0.93*	0.67	*1.00*	0.44	*1.00*	0.33	0.61
Ante_SM	0.13	0.74	0.38	*0.90*	0.79	*1.00*	0.63	*0.96*	*0.83*	*0.99*	*0.90*	*0.95*	0.50	*0.89*	0.19	0.59	*1.00*	0.70
Ante_AET	0.09	*0.81*	0.27	0.31	0.31	0.60	0.20	0.72	0.33	0.10	0.42	0.48	0.42	0.30	0.14	0.61	0.33	*1.00*
Post_Q	0.41	0.07	0.21	0.27	0.18	*1.00*	0.16	0.77	0.66	*0.80*	0.17	*0.81*	0.42	0.10	0.32	0.37	*1.00*	0.63

Note: Posterior inclusion probability >= 0.8 in italic.

Table C46.: Comparison between BMA performance using rainfall/runoff predictors only and all candidate predictors (full models).

Constituent	NSE for Cluster 1 ("wet")			NSE for Cluster 2 ("dry")		
	Rainfall, runoff only	Full model	% change in NSE	Rainfall, runoff only	Full model	% change in NSE
TSS	0.32	0.35	11	0.42	0.58	38
PN	0.32	0.40	24	0.38	0.59	56
NO_X	0.23	0.49	113	0.32	0.64	101
NH_4	0.00	0.39	/	0.18	0.34	88
DON	0.20	0.37	84	0.20	0.43	117
FRP	0.27	0.45	68	0.26	0.40	56
DOP	0.00	0.04	/	0.22	0.62	181
PP	0.29	0.36	24	0.34	0.51	51
EC	0.41	0.68	66	0.39	0.54	39

Table C7. Performance statistics for nine constituents for the modelled and observed temporal variability, according to Moriasi et al. (2015).

Constituent	Cluster one	Cluster two
TSS	Indicative	Satisfactory
PN	Satisfactory	Satisfactory
NO_X	Satisfactory	Good
NH_4	Satisfactory	Indicative
DON	Satisfactory	Satisfactory
FRP	Satisfactory	Satisfactory
DOP	Indicative	Good
PP	Satisfactory	Satisfactory
EC	Satisfactory	Satisfactory